INTERNATIONAL SCIENTIFIC JOURNAL
GEOGRAPHICA PANNONICA
Volume 29, Issue 2, 149–171 (June 2025)
Journal homepage: http://www.dgt.uns.ac.rs/en/homepage/pannonica/

Multiscale Analysis of Green Infrastructure Impacts on PM2.5 and PM10 Pollution in Delhi, India

Atul Kumar[A*], Mahua Mukherjee[A], Ajanta Goswami[A], Nishant Saxena[A], Aditya Rahul[B]

[A] *Indian Institute of Technology Roorkee; Roorkee, Uttarakhand, Republic of India*
[B] *Trinity College Dublin, the University of Dublin, College Green, Dublin, Republic of Ireland*

KEYWORDS

- Green Infrastructure (GI)
- PM2.5
- PM10
- Green Infrastructure Characteristics
- Urban Air Quality
- NDVI
- PCA
- FRAGSTAT

ABSTRACT

Urban air pollution, particularly from fine particulate matter (PM2.5 and PM10), poses critical environmental and public health challenges in rapidly urbanizing regions. This study presents a multiscale, seasonal analysis of the relationship between Green Infrastructure (GI) landscape characteristics and PM concentrations in Delhi, India. Using high-resolution Sentinel-2 imagery (2019–2021) and air quality data from 39 Central Pollution Control Board (CPCB) monitoring stations, we quantified 15 GI characteristics across five spatial scales (0.5–2.5 km) using NDVI. Empirical Bayesian Kriging was applied for spatial interpolation of PM values, and Otsu's thresholding was used to delineate vegetated areas. Principal Component Analysis (PCA) and regression models revealed that compositional metrics—such as Class Area (CA) and Percentage of Landscape (PLAND)—showed consistent negative correlations with PM2.5 and PM10 levels across all scales and seasons. Configuration metrics, including Largest Patch Index (LPI), Edge Density (ED), and Aggregation Index (AI), exhibited scale- and season-specific influences, with stronger effects observed at broader spatial scales during winter and autumn. The findings suggest that both the quantity and spatial arrangement of urban vegetation significantly affect local air quality. The study underscores the need for scale-aware, evidence-based GI planning as a nature-based solution, supporting India's airshed-level approach to urban pollution management. These insights offer practical guidance for urban policymakers and planners aiming to enhance air quality through strategic green infrastructure design.

Introduction

The globe saw an upsurge in human populations during the Industrial Revolution in the nineteenth century, which has exacerbated the pace of urbanization since then (Grimm et al., 2008; Singh et al., 2020). Countries' population projections report that over 95% of the global population's net growth occurs in the cities of developing countries (Jiang & O'Neill, 2017; UNDESA, 2019). In addition, nearly all of the world's new megacities (defined as having a population of more than 10 million people) are located in the developing world (UNDESA, 2019). Globally, rapid economic expansion and unregulated urbanisation have altered land surface attributes, including roughness, thermal inertia, and albedo (AlKhaled et al., 2020; Zhou et al., 2019). Such factors further impact regional meteorological parameters like temperature, wind speed, and air quality (Agarwal & Tandon, 2010; Grimm et al., 2008). In recent decades, fast economic expansion and unregulated urbanization have brought unprecedented negative an-

* Corresponding author:Atul Kumar; e-mail: akumar5@ar.iitr.ac.in
doi: 10.5937/gp29-53959
Received: October 10, 2024| Revised: June 2, 2025| Accepted: June 26, 2025

thropogenic stress in the urban environment regarding air quality, which has become a growing concern in densely populated regions of developed as well as developing countries (Singh et al., 2020; Song et al., 2018; Molina et al., 2012; Impacts, n.d.; Mathers et al., 1999). Megacities usually have significant PM10 and PM2.5 levels from fossil fuel combustion, fugitive dust, and biomass burning from industry, transportation, and densely populated areas. The WHO reported that outdoor air pollution (PM) kills about 4 million people yearly, accounting for 11.65% of worldwide deaths (WHO, 2018). Air pollution, the most significant health concern posed by the environment, is costing the world a total of $8.1 trillion, which is comparable to 6.1% of the global GDP (Li, 2016; UNEP, 2018; Li, 2017; Molina et al., 2012). Throughout the 1950s and 1960s, Particulate Matter (PM) pollution experienced a notable expansion in European and North American locations. Its severity, meanwhile, has been rising in developing countries, including India and China (Rohde & Muller, 2015; Yale & Columbia Universities, 2022). In India, during the last decades, air pollution in urban regions has become a major urban environmental issue (Gulia et al., 2015a; Chelani et al., 2001; Ramani et al., 2019; Central Pollution Control Board, 2003; Gupta, 2008; Ministry of Environment & Forests, 1987; Kushwaha & Nithiyanandam, 2019; Menon & Sharma, 2021; Ramaiah & Avtar, 2019; Kotharkar & Bagade, 2018). The 2021 assessment by IQAir, a Swiss organisation that assesses air quality by measuring PM concentration, placed India as the fifth most polluted nation out of 117 countries. It also identified Delhi as the most significant metropolitan agglomeration with the most hazardous air in the world (IQAir, 2021). In India, it has been estimated that the average economic impact of PM air pollution alone amounts to 5.4 per cent of the country's yearly GDP (Greenpeace, 2020). Furthermore, it is accountable for roughly one million deaths each year and contributes to 980,000 preterm births (Chatterji, 2020). It is estimated that in 2021, the deaths of 40,000 children under the age of five were directly linked to PM pollution (IQAir, 2021). According to studies conducted during the COVID-19 pandemic, being exposed to particulate matter (PM2.5 & PM10) increases the likelihood of acquiring the virus and experiencing more severe symptoms, including mortality, if infected (Role, 2021; Soni, 2021). The effects of urban issues extend to the urban, regional, continental, and global scales. Large cities pose challenges in managing a rising population, yet they also pose potential opportunities to manage environmental issues such as air pollution sustainably.

In the last 20 years, extensive research has been conducted on PM10 and PM2.5, which are typically considered harmful to people's health (Kumar et al., 2019; Mannucci et al., 2015; Leão et al., 2023; Ramadan et al., 2025). A number of studies examined the relationship between PM pollution and human health, finding that it was associated with sharp rises in respiratory and cardiovascular diseases (Morelli et al., 2016; Lavigne et al., 2016; Peters, 2011; Sangkham et al., 2024). Numerous studies have examined the spatial distribution of particulate matter of varying sizes at regional or national scales, along with the influencing variables (Sharma et al., 2014; Luo et al., 2020). Source apportionment of particles is another crucial field of study focused on characterizing different sources of fine-particulate air pollution (Banerjee et al., 2015; Sharma et al., 2014; Guttikunda et al., 2014; Nautiyal et al., 2025; Meng et al., 2025). Global cities have studied and suggested many ways to lower PM pollution. These include using cleaner energy, changing the way the economy grows, limiting driving, and working together at the regional or national level (Guttikunda et al., 2019; Gulia et al., 2015b; Dhingra, 2020; Wu et al., 2017). Identifying sustainable approaches by using nature-based solutions by which PM pollution can be reduced nowadays has become a priority for researchers and urban planners (Zhang et al., 2024; Power et al., 2023; Tomson et al., 2025). For example, research in 10 US cities found that trees eliminated 4.7 t to 64.5 t of PM2.5 yearly (Nowak et al., 2006). Similarly, Leicester, UK, research found that trees and grasses remove 14 tons of PM2.5 annually (Jeanjean et al., 2016; Jeanjean et al., 2017). Local PM declines were detected in Sydney's urban woodlands by Irga et al. (2015). Mcdonald et al. (2007) simulated PM10 concentrations in the West Midlands and Glasgow (UK) and showed that tree cover might cut PM by 10%. Kumar et al. (2019) suggested in their study that green infrastructure (GI) as a physical barrier may lower PM10 by 60%, 59%, 16%, 63%, and 77% compared to control circumstances. Due to the preponderance of qualitative research and the scarcity of quantitative studies, much of the attention is placed on a micro-scale configuration and species typology of green infrastructure (Yu & Jingyi, 2019; Im, 2019; Bartesaghi-Koc et al., 2018; Ouyang et al., 2021; Urban Climate Lab, 2016). Recently, there has been growing interest in understanding how the landscape level or urban macro scale composition and configuration of green infrastructure (GI) affect the delivery of ecosystem services, including pollution control (Andersson-Sköld et al., 2018; Selmi et al., 2016; Wu et al., 2018; Lei et al., 2018; Lei et al., 2021; Ramyar & Zarghami, 2017; Tomson et al., 2025; Barwise, 2023; Yao et al., 2025). "Green Infrastructure" (GI) is a natural and semi-natural open place around cities that provides ecological services to the surroundings (Calfapietra et al., 2019; Bartesaghi-Koc et al., 2019; NWGITT, 2008; Ramyar & Zarghami, 2017). GI is a novel name, but its concept originates in planning and conservation initiatives dating back 150 years. The concept was prompted by two precedents: integrating parks and other green spaces for people and linking natural areas to improve biodiversity and reduce habitat fragmentation (Benedict et al., 2006; Schneekloth, 2000; US EPA, OW, 2010;

Tallis et al., 2015; Sinnett et al., 2015; Calfapietra & Cherubini, 2019). To investigate and quantify the effects of GI on many sustainability advantages, researchers have attempted to develop a general categorisation of GI based on multiple benefits through quantitative and qualitative studies at local to regional scales. GI at the regional scale can have substantial spatial heterogeneity because various land cover and land-use types exhibit distinctive surface features. In urban form and urban landscape study, landscape metrics are algorithms that measure patches, classes, and aggregation of landscape patterns (Zheng et al., 2020; Wu et al., 2015; Lei et al., 2018; Ahern, 2007; Fan et al., 2015; Guo et al., 2021). Landscape metrics may efficiently illustrate the GI characteristics (Mcgarigal, 2015). They have been extensively utilised to explore the patterns of greenspace landscapes and their effects on PM reduction (Lei et al., 2021; Guo et al., 2021; Lei et al., 2018; Wu et al., 2015; Myint et al., 2015).

Recent studies have shown that the fragmentation of urban greenspace has a significant impact on particulate matter pollution. An investigation conducted by Lei et al. in a Chinese metropolis indicated that the composition of greenspace had a more significant impact on lowering PM pollution at shorter distances. In contrast, the configuration of greenspace was more significant at longer distances (Lei et al., 2018; Lei et al., 2021; Barwise, 2023). Further, a study demonstrated, that PM2.5 concentration and landscape evenness/fragmentation are strongly connected (Wu et al., 2015; Barwise, 2023; Zhang et al., 2024). There are limited or no studies on particulate matter pollution in relation to green infrastructure landscape patterns in Indian cities. Most, if not all, of these studies, adopted a FRAGSTAT model, which represents a landscape in three levels of matrices, i.e., patch, class, and landscape metrics, with further segmentation in area-edge, shape, and aggregations (Forman, 1995; McGarigal, 1995; McGarigal et al., 2002; Cao et al., 2024; Jiang et al., 2023). This study aims to propose landscape-level Green Infrastructure (GI) as a potentially sustainable approach to explain the variation of the seasonal PM concentration in an urban area. The study has direct alignment with the government approach of managing air quality and urban risk at the air-shed level contrary to the local scale by integrating green infrastructure as a potential nature-based solutions (CleanAirAsia, 2016; CPCB, 2013). The objectives of this study were to investigate the relationship between the landscape pattern of GI and PM concentration at multiple scales. The contributions of this study include the following: it investigates the role of green infrastructure composition and configuration in indicating particulate matter concentration in Delhi; it offers recommendations for the green infrastructure planning of urban redevelopment in the city.

Materials and Methodology

Study Area

The city is noted for its air pollution, with air quality levels routinely surpassing the World Health Organization's recommended thresholds, creating significant health hazards for its inhabitants (REF: IQ Air 2023). The World Health Organization (WHO) produced a report in 2014 identifying Delhi as the most polluted city in the world, citing air pollution as the city's most pressing problem (Saraswat et al., 2017; Jalan, 2019; Jain et al., 2021; Guttikunda & Calori, 2013). The Delhi government has taken various initiatives for long-term and seasonal measures to combat air pollution. For example, the Graded Response Action Plan (GRAP) developed by the Central Pollution Control Board (CPCB), the odd-even vehicle policy in 2016. The government also periodically shut down coal-based thermal power facilities and developed real-time air monitoring devices and the Green Delhi App for citizens to report pollution levels. In addition to regulatory and technological measures, the Delhi government has increasingly adopted nature-based solutions to combat air pollution and improve urban resilience. The Delhi Development Authority (DDA) and Forest Department have created additional city forests and green belts to filter air and cool the city. They have also pushed vertical gardens and green walls along flyovers and metro pillars to provide vegetation to crowded urban areas. The government intended to maximise the potential of green infrastructure by implementing several programmes like the smart city mission, the India Forum for Nature-based Solutions, the AMRUT project, etc. Delhi has undergone unprecedented urbanisation over the past few decades and manifested high GI and air pollution heterogeneity. Thus, Delhi serves as a good model for addressing the following questions: (1) Do the GI landscape patterns affect the Particulate matter concentration level? Furthermore, (2) if so, how do the PM10 or PM2.5 vary by different GI spatial patterns and scales?

Data

PM2.5/10 Measurements: 39 Air Quality Monitoring Stations (AQMS) are deployed throughout the city, as shown in Figure 1. All the stations are uniformly distributed in the city. These monitoring stations provide hourly and daily mean PM2.5/10 pollution concentration data. The data protocol suggests that each monitoring station has a spatially representative radius of 1 to 5 sq. km (CPCB, 2015). These AQMS are located at a height of 3 to 15 m on the street or roadsides. PM2.5/10 concentration and weather data at all 39 AQMS from the year 2019 to 2021 were obtained from

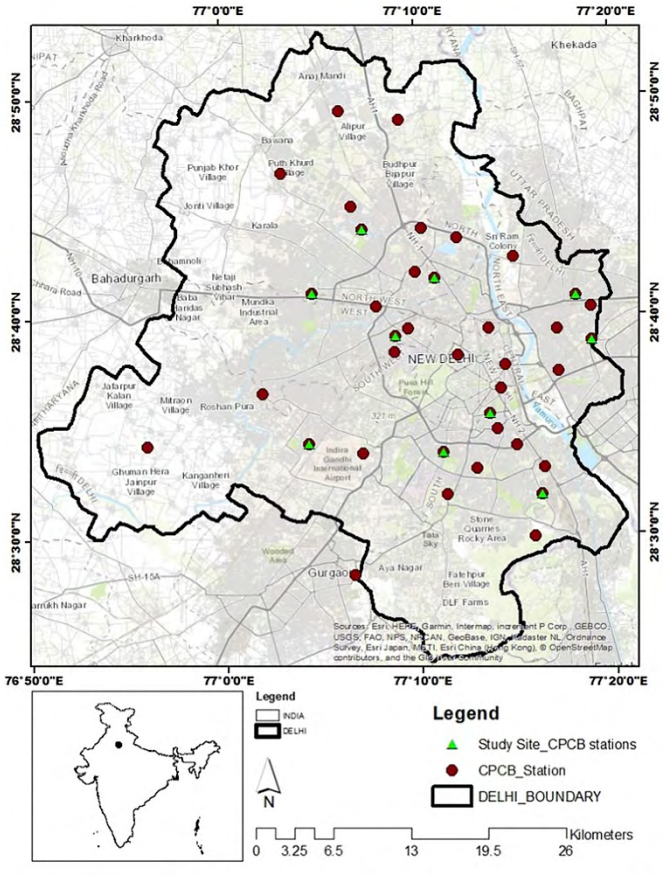

Figure 1. Delhi city Boundary and Location of all CPCB monitoring stations in Delhi and Location of monitoring stations selected for the study

the Central Pollution Control Board (https://app.cpcbccr.com/ccr/#/caaqm-dashboard-all/caaqm-landing). Seasonal mean data sets for the PM concentration were calculated based on the respective months of the seasons. Geographical Information System (GIS) based interpolation techniques have been used to map the concentration of particulate matter in interest. The interpolation technique is used to predict values in the cells in a raster when there are limited sample data points (Shareef et al., 2016; Bezyk et al., 2021; Singh & Tyagi, 2013a; Londoño-Ciro & Cañón-Barriga, 2015).The study used geostatic analysis interpolation techniques called Empirical Bayesian kriging; this method estimates cell values by averaging the sample point value in the neighbourhood of each processing cell. The standardised R square value for the maps is between 0.94 and 0.99. Data-driven traditional Empirical Bayesian kriging predicts unsampled locations. Parallel processing helps Empirical Bayesian kriging forecast large datasets and improve prediction accuracy. The method can provide accurate and reliable predictions of geographical data.

Green Infrastructure (GI) characterization

GI in an urban region, including land surfaces covered by trees, shrubs, and herbaceous vegetation, has long been known to influence local atmospheric PM concentrations and Temperature. GI changes PM concentrations through direct and indirect ways (Hofman et al., 2016) at plant level and landscape level, including capturing particulates on leaf surfaces (Zhang et al., 2021b)cities are implementing greening plans to satisfy the demands of residents for a more habitable environment. Because the relationship between the supply and demand of ecosystem services (ESs and altering urban temperature, atmospheric turbulence, and wind flow through "evapotranspiration" (Soydan, 2020; Liu & Shen, 2014). To obtain the landscape patterns of GI, which are reported in several scholarly works, 10 m spatial resolution data of Sentinel-2 (Year 2019, 20202 and 2021) from the Google Earth engine repository is used to delineate normalized difference vegetation index (NDVI) for 2019, 2020, and 2021; the study used the mean season-wise data for the specific month of the respective years. NDVI is a popular way to measure the cover and condition of vegetation in urban areas using remote sensing (Thiis et al., 2018). The threshold values of the seasonal NDVI maps were calculated using Otsu's thresholding technique, defining the condition of vegetative cover (Grover & Singh, 2015; Gašparović & Dobrinić, 2021; Ashok et al., 2021). Otsu's approach minimises vegetation and non-vegetation pixel variation (Dissanayake et al., 2018)(Sathyakumar et al., 2020). The difference between near-infrared and red-light reflectance is used to calculate NDVI values ranging from -1 to 1. Otsu's approach analyses histograms of NDVI values to identify an appropriate threshold t that divides pixel values into vegetation and non-vegetation classes. This is done by finding a threshold value that maximizes class variance $\sigma^2_b(t)$, defined as $\sigma^2_b(t) = \omega_1(t)\omega_2(t)[\mu_1(t)-\mu_2(t)]^2$, where $\omega_i(t)$ and $\mu_i(t)$ are the class probabilities and means of the two classes separated by threshold t. Finally, the resulting binary classification designates non-vegetation as pixels with NDVI < t and vegetation as pixels with NDVI ≥ t. It adjusts to the data patterns of each scene, making it strong for extensive or automated vegetation mapping without needing manual set limits for NDVI-based land cover analysis. After selecting the optimal threshold value mentioned in Table 1, binaries the image by putting all pixels with intensity levels over the threshold into the vegetation while converting all other pixels into the non-vegetation class (Sathyakumar et al., 2020). Finally, landscape-level metrics measured GI landscape composition and configuration features. Landscape-level metrics were widely used to describe GI patterns (Lei et al., 2018; Heather R. McCarthy, 2011; Mcgarigal, 2015). In this study, fifteen landscape-level metrics were used to measure landscape patterns of GI, as listed in Table 2. The landscape patterns included five composition metrics and ten configuration metrics (McGarigal, 1995). These metrics have been utilised in various landscape pattern-ecological process articles (Zhou et al., 2011; Li et al.,

2013; Chen et al., 2019; Wu et al., 2018; Liang & Gong, 2020; Soydan, 2020). These parameters were selected based on three criteria: (1) theoretically and practically significant; (2) readily computed and explained; and (3) minimum repetition.

FRAGSTATS was used to quantify landscape metrics using NDVI maps for ten plots. In this study, we used CPCB's ten air quality monitoring stations (AQMS) as central points to create five square plots per site ranging in size from 0.5 km x 0.5 km to 2.5 km x 2.5 km for each monitoring site, as shown in Figure 2. The following were taken into consideration while choosing the locations: (i) choosing monitoring sites with consistently high pollution levels (all seasons), (ii) avoiding areas with water bodies or other potential modifiers, (iii) Unique Local Climate Zone (built-up morphology) with variables land use and (iv) there was no primary emission source present. The smallest sample plot is 0.5 km x 0.5 km, which is ideal for urban micro-scale urban forestry study, while 2.5 km x 2.5 km is ideal for urban local scale. NDVI maps were validated using 100 randomly chosen points and reference data from Google images; the confusion matrix suggests 92% seasonal average accuracy with a seasonal average kappa coefficient value of 94% for the vegetation classifications. Finally, the seasonal data sets of the PM (PM10, PM2.5) concentration, along with the quantified GI landscape characteristics, were employed in the Principal Component Analysis (PCA) to analyse the variation of variables. PCA is a statistical technique commonly used in environmental studies to identify key factors by isolating those that account for the most variance in the data.

Table 1. Season-wise threshold value for Binarization of NDVI Image

Season	Threshold value for Binarization of NDVI Image
Summer (April to June)	0.29
Monsoon (July to August)	0.17
Autumn (September to October)	0.29
Winter (November to January)	0.17
Spring (February to March)	0.24

Data analysis

Green infrastructure features that have similar properties are clustered together using a hierarchical cluster analysis method (Yu et al., 2017; Grafius et al., 2018). Then, at first, we performed a one-way analysis of variance (ANO-

Table 2. Green Infrastructure characterization at landscape level

Typology	Metrics Type	GI Characterization	Equation (Unit)
Composition	Area	CA	$CA = \sum_{j=1}^{n} a_{ij}\left(\frac{1}{10{,}000}\right)$
		PLAND	$PLAND = P_i \frac{\sum_{j=1}^{n} a_{ij}}{A}(100)$
		LPI	$LPI = \frac{max\left(a_{ij}\right)}{A}(100)$
	Shape	SH_MN	$SH\_MN = \frac{1}{n} X \sum_{i=1}^{n} \frac{e_i}{min e_i}$
		LSI	$LSI = \frac{.25E^*}{\sqrt{A}}$
Configuration	Aggregation	COH	$COH = \left[1 - \frac{\sum_{j=1}^{n} P_{ij}^*}{\sum_{j=1}^{n} P_{ij}^* \sqrt{a_{ij}^*}}\right]\left[1 - \frac{1}{\sqrt{Z}}\right]^{-1} \cdot (100)$
		NP	$NP = n_i$
		PD	$PD = \frac{N}{A}(10{,}000)(100)$

Typology	Metrics Type	GI Characterization	Equation (Unit)
Configuration	Aggregation	CLUMPY	$CLUMPY = \begin{cases} \frac{G_i - P_i}{1 - P_i} \; for \; G_i \geq P_i \\ \frac{G_i - P_i}{1 - P_i} \; for \; G_i < Pi; P_i \geq 0.5 \\ \frac{P_i - G_i}{-P_i} \; for \; G_i < Pi; P_i \geq 0.5 \end{cases}$
		ENN_MN	$ENN\_MN = d(in\ km)$
		AI	$AI = \left[\sum_{i=1}^{m}\left(\frac{g_{ii}}{max\ g_{ii}}\right)P_i\right](100)$
		SDI	$SDI = -\sum_{i=1}^{m}(P_i \cdot \ln P_i)$
		SEI	$SEI = \frac{-\sum_{i=1}^{m}(P_i \cdot \ln P_i)}{\ln m}$
		ED	$ED = \frac{E}{A}(10{,}000)$
		TE	$TE = E$

Note: TOTAL AREA (CA); PERCENTAGE OF LANDSCAPE (PLAND); LARGEST PATCH INDEX (LPI); MEAN SHAPE INDEX (SH_MN); LARGEST SHAPE INDEX (LSI); PATCH COHESION INDEX (COH); NUMBER OF PATCH (NP); PATCH DENSITY (PD); CLUMPINESS (CLUMPY); MEAN NEAREST NEIGHBOR DISTANCE (ENN_MN); AGGREGATION INDEX (AI); SHANNON'S DIVERSITY INDEX (SDI); SHANNON'S EVENNESS INDEX (SEI); TOTAL EDGE (TE); EDGE DENSITY (ED); (ref: McGarigal, 1995; McGarigal, 2003)

VA) to examine whether there were significant differences among the PM2.5 and PM10 concentrations among the four seasons (Ginevan & Splistone, 2004; Vieira et al., 2018; Wu et al., 2018). We compared the PM2.5 and PM10 concentrations using the least significant difference test, with a significance level of $p < 0.05$. All values were reported as mean ± standard error. Second, we used the principal component analysis (PCA) to investigate the relationship between the PM2.5/10 concentration with the characterise and quantified green infrastructure at landscape level at scale variation from micro (0.5 km x 0.5 km) to local (2.5 km x 2.5 km) urban scale. PCA is the preferred approach for studying variation in environmental parameters with vegetation (Zhang et al., 2016; Yang et al., 2011; Ou et al., 2017; Andrew et al., 2012; Wu et al., 2018; Elhaik, 2022). It can help researchers understand the underlying ecological processes that drive these interactions. In addition, it can help to assess the GI composition and configuration impact on environmental variables such as PM2.5/10 (Chen & Dai, 2022; Heo et al., 2020), and assist in determining environmental factors variation in relation to quantified GI patterns (Wu et al., 2018; Jolliffe et al., 2016). It has been utilised in ecological research in tropical forests, grasslands, and wetlands to examine the link between GI and environmental factors (Kenkel, 2006; Yang et al., 2011; Rezaei & Millard-Ball, 2023). Climate change, land use change, and other anthropogenic disturbances have also been studied using it (Franklin et al., 1995; Jolliffe et al., 2016; Vieira et al., 2015). Finally, PCA regression was used to evaluate the relative impact of the five-composition measures and ten-configuration metrics of explanatory variables on PM2.5/10 concentration at each scale.

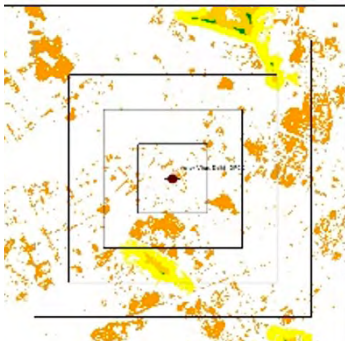

(A-1)

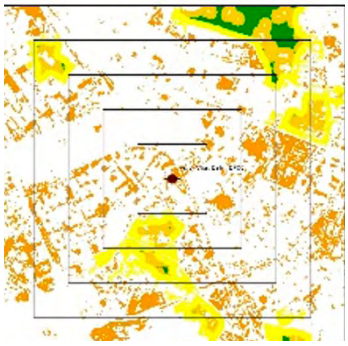

(B-1)

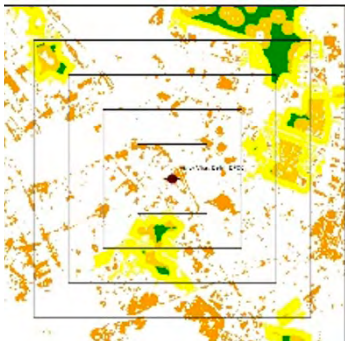

(C-1)

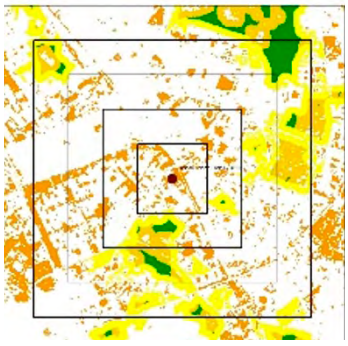

(D-1)

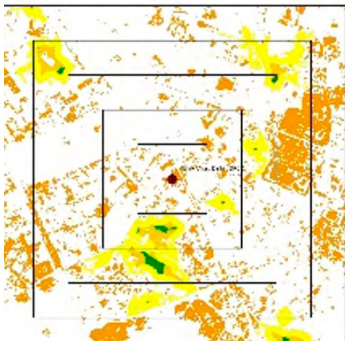

(E-1)

Google Earth Image of the site Ashok Vihar (Delhi) Monitoring Stations

Green Infrastructure Characterization mapping for all the seasons and multiscale buffer at Ashok Vihar (Delhi) Monitoring Stations

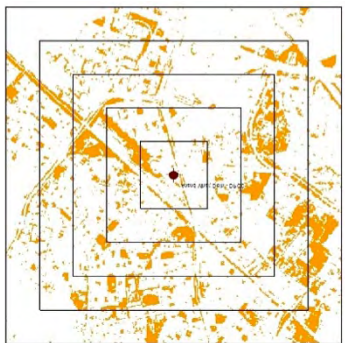

(A-2)

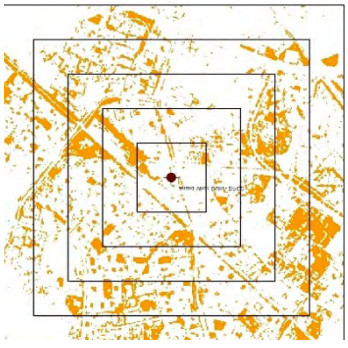

(B-2)

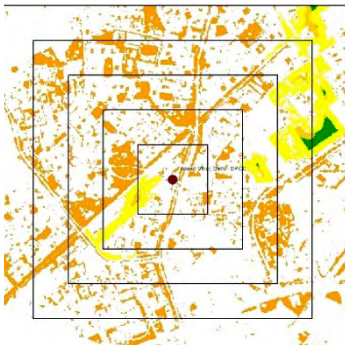

(C-2)

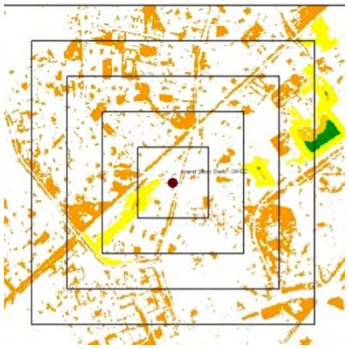

(D-2)

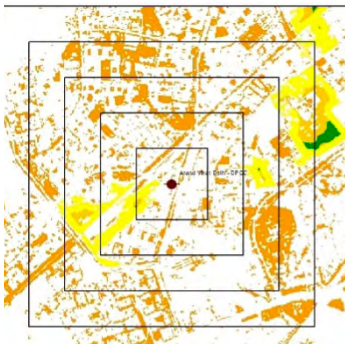

(E-2)

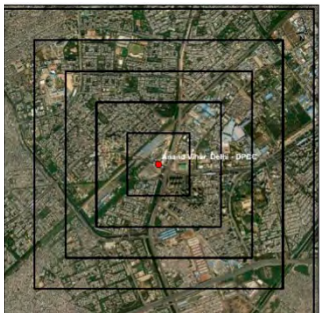

Google Earth Image of the site Anand Vihar (Delhi) Monitoring Stations

Green Infrastructure Characterization mapping for all the seasons and multiscale buffer at Anand Vihar (Delhi) Monitoring Stations

Figure 2. GI characterisation mapping for the selected study site in Delhi and buffer region depicting 0.5km (the inner square plot), 1km, 1.5km, 1.5km, 2km, and 2.5km (the outer square plot), A1-10: Spring Season; B1-10: Summer Season; C1-10: Monsoon Season; D1-10: Autumn Season; E1-10: Winter Season

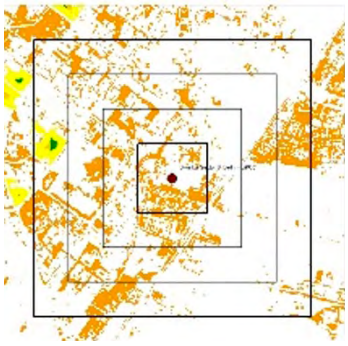

(A-3)

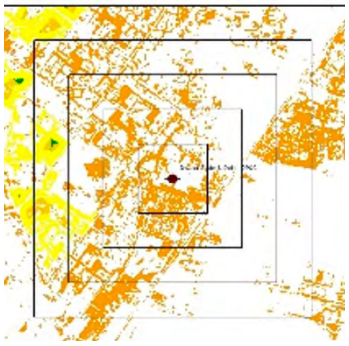

(B-3)

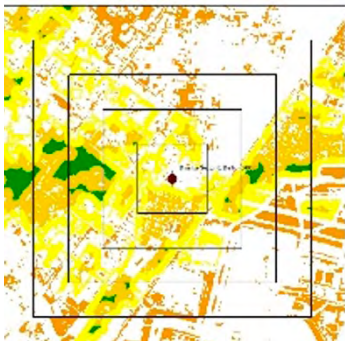

(C-3)

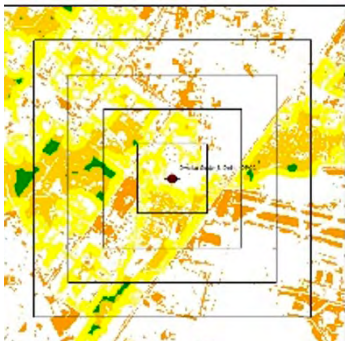

(D-3)

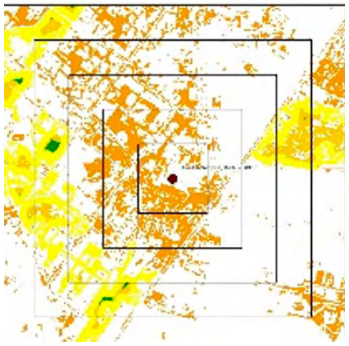

(E-3)

Google Earth Image of the site Dwarka-Sector 8 (Delhi) Monitoring Stations

Green Infrastructure Characterization mapping for all the seasons and multiscale buffer at Dwarka-Sector 8 (Delhi) Monitoring Stations

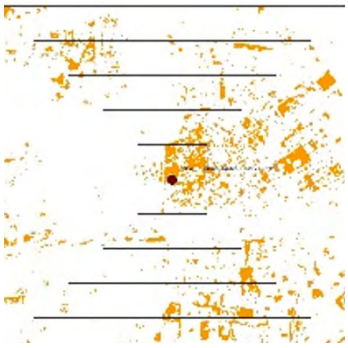

(A-4)

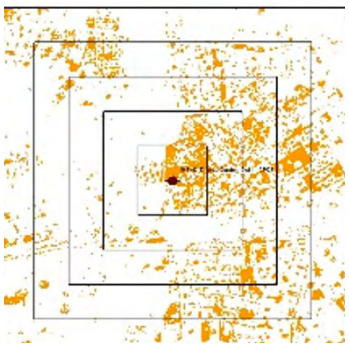

(B-4)

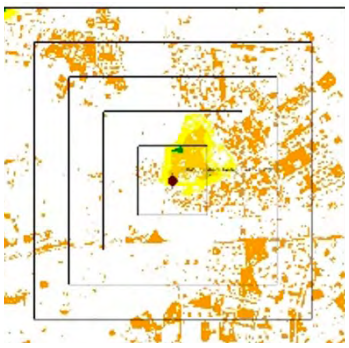

(C-4)

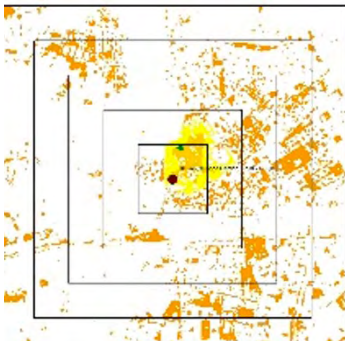

(D-4)

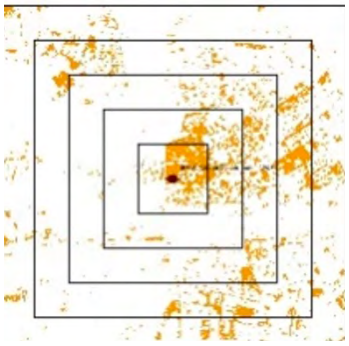

(E-4)

Google Earth Image of the site IHBAS, Dilshad Garden (Delhi) Monitoring Stations

Green Infrastructure Characterization mapping for all the seasons and multiscale buffer at IHBAS, Dilshad Garden (Delhi) Monitoring Stations

Figure 2. GI characterisation mapping for the selected study site in Delhi and buffer region depicting 0.5km (the inner square plot), 1km, 1.5km, 1.5km, 2km, and 2.5km (the outer square plot), A1-10: Spring Season; B1-10: Summer Season; C1-10: Monsoon Season; D1-10: Autumn Season; E1-10: Winter Season (continued)

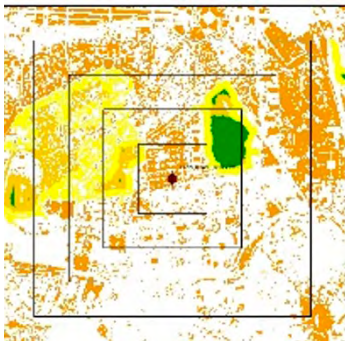

(A-5)

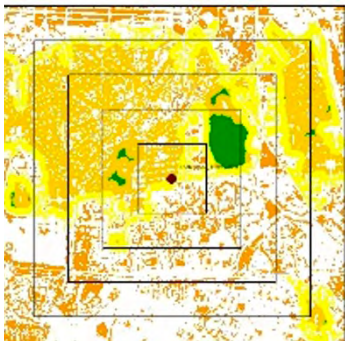

(B-5)

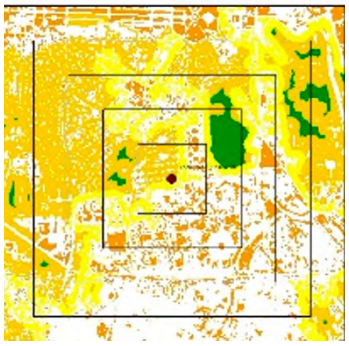

(C-5)

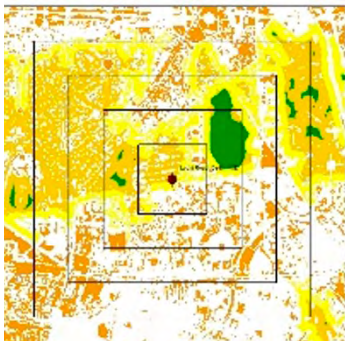

(D-5)

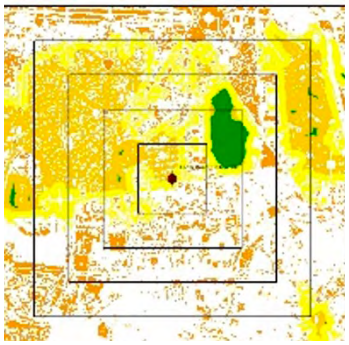

(E-5)

Google Earth Image of the site Lodhi Road (Delhi) Monitoring Stations

Green Infrastructure Characterization mapping for all the seasons and multiscale buffer at Lodhi Road (Delhi) Monitoring Stations

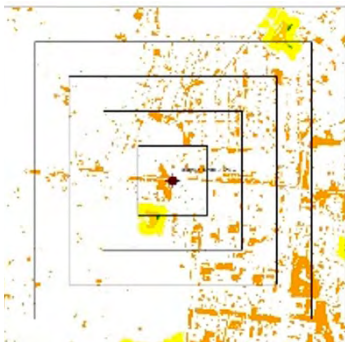

(A-6)

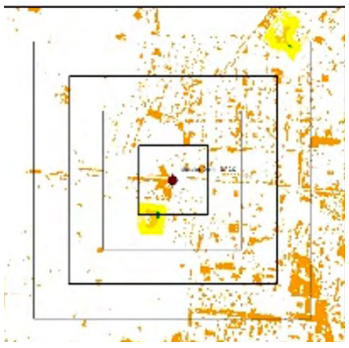

(B-6)

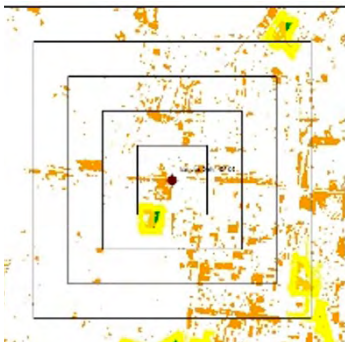

(C-6)

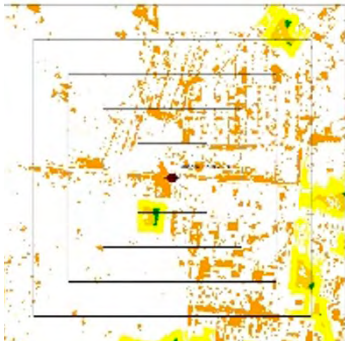

(D-6)

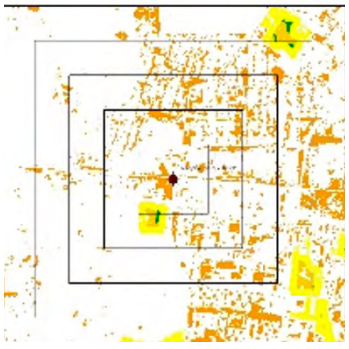

(E-6)

Google Earth Image of the site Mundka (Delhi) Monitoring Stations

Green Infrastructure Characterization mapping for all the seasons and multiscale buffer at Mundka (Delhi) Monitoring Stations

Figure 2. GI characterisation mapping for the selected study site in Delhi and buffer region depicting 0.5km (the inner square plot), 1km, 1.5km, 1.5km, 2km, and 2.5km (the outer square plot), A1-10: Spring Season; B1-10: Summer Season; C1-10: Monsoon Season; D1-10: Autumn Season; E1-10: Winter Season (continued)

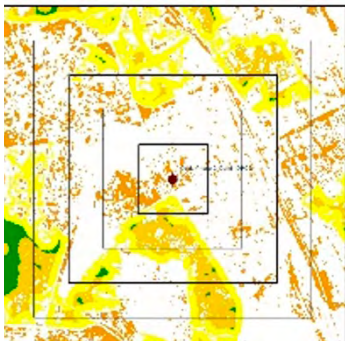

(A-7)

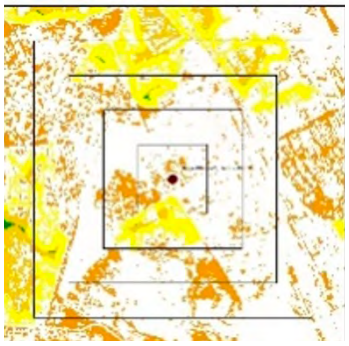

(B-7)

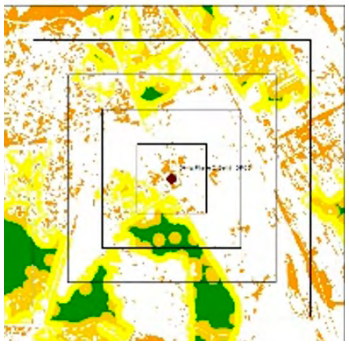

(C-7)

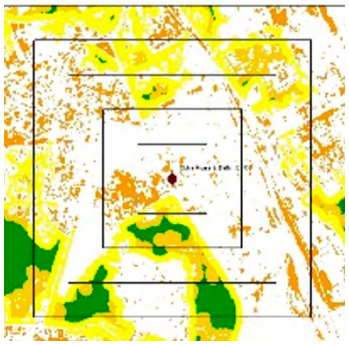

(D-7)

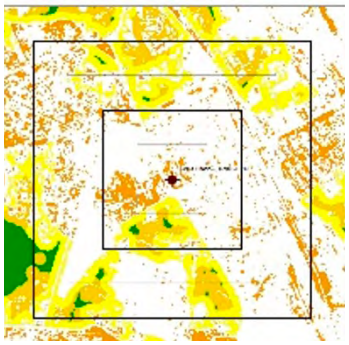

(E-7)

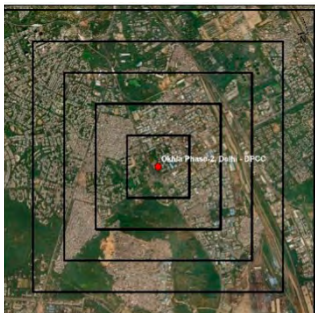

Google Earth Image of the site Okhla Phase-2 (Delhi) Monitoring Stations

Green Infrastructure Characterization mapping for all the seasons and multiscale buffer at Okhla Phase-2 (Delhi) Monitoring Stations

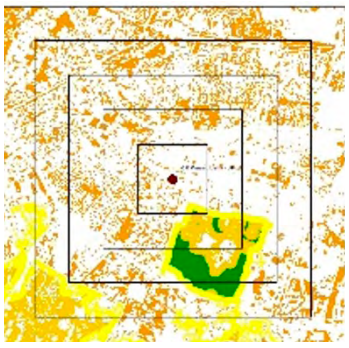

(A-8)

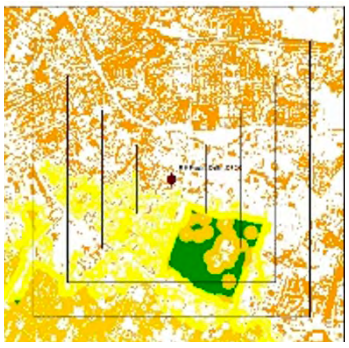

(B-8)

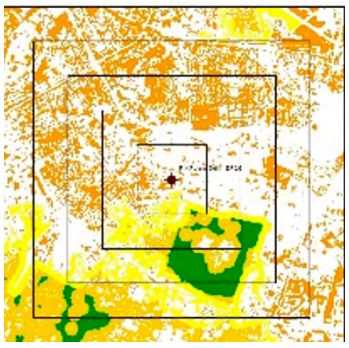

(C-8)

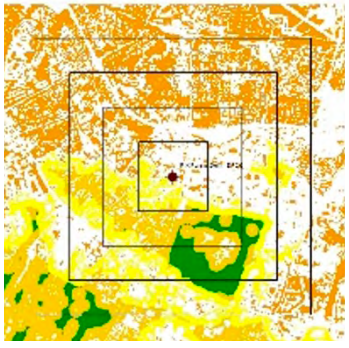

(D-8)

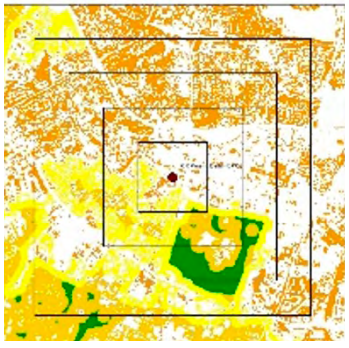

(E-8)

Google Earth Image of the site R K Puram (Delhi) Monitoring Stations

Green Infrastructure Characterization mapping for all the seasons and multiscale buffer at R K Puram (Delhi) Monitoring Stations

Figure 2. GI characterisation mapping for the selected study site in Delhi and buffer region depicting 0.5km (the inner square plot), 1km, 1.5km, 1.5km, 2km, and 2.5km (the outer square plot), A1-10: Spring Season; B1-10: Summer Season; C1-10: Monsoon Season; D1-10: Autumn Season; E1-10: Winter Season (continued)

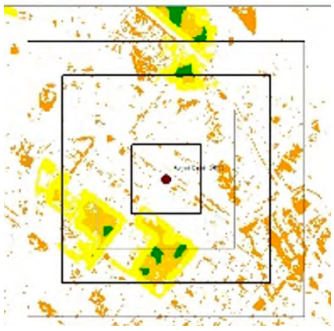

(A-9)

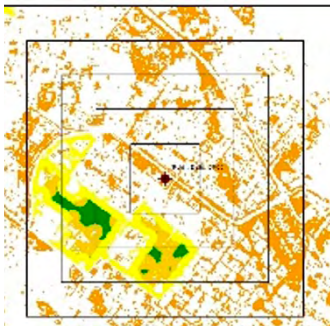

(B-9)

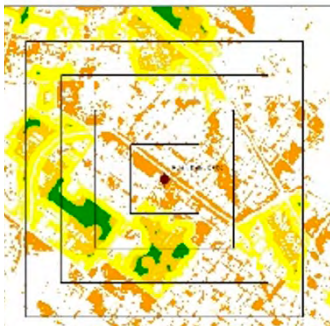

(C-9)

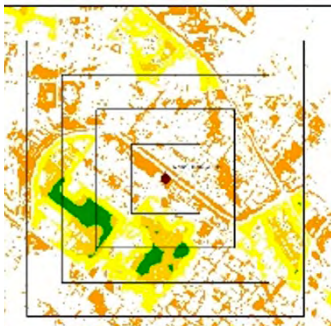

(D-9)

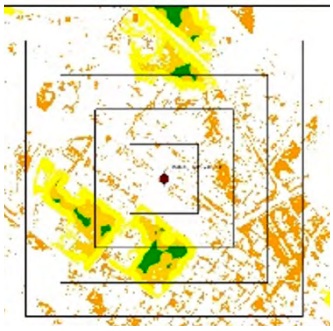

(E-9)

Google Earth Image of the site Rohini (Delhi) Monitoring Stations

Green Infrastructure Characterization mapping for all the seasons and multiscale buffer at Rohini (Delhi) Monitoring Stations

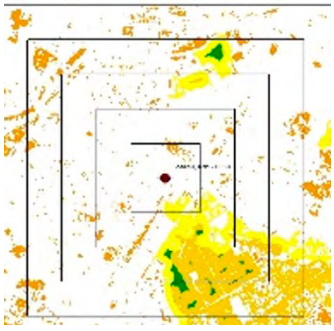

(A-10)

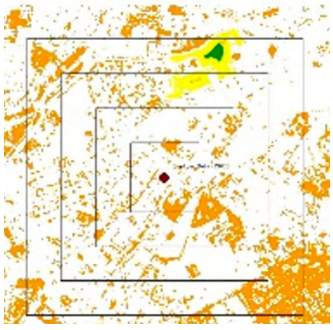

(B-10)

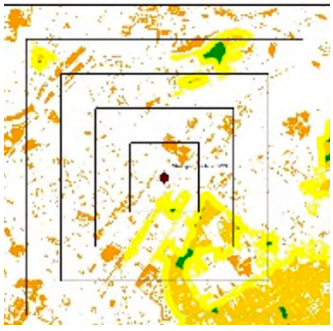

(C-10)

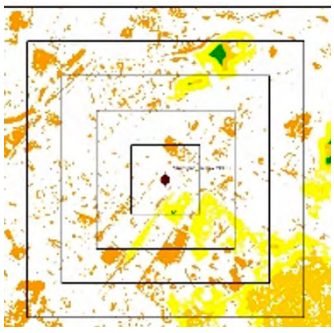

(D-10)

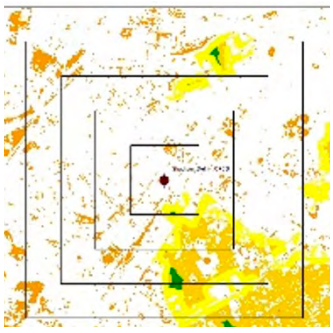

(E-10)

Google Earth Image of the Shadipur (Delhi) Monitoring Stations

Green Infrastructure Characterization mapping for all the seasons and multiscale buffer at Shadipur (Delhi) Monitoring Stations

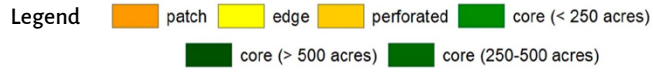

Figure 2. GI characterisation mapping for the selected study site in Delhi and buffer region depicting 0.5km (the inner square plot), 1km, 1.5km, 1.5km, 2km, and 2.5km (the outer square plot), A1-10: Spring Season; B1-10: Summer Season; C1-10: Monsoon Season; D1-10: Autumn Season; E1-10: Winter Season (continued)

Result

Clustering GI characteristics

Landscape metrics are often directly deployed as independent variables to explore the effects of landscape patterns on air pollution. Many of these metrics exhibit strong correlations; therefore, certain metrics must be excluded from the full model to prevent multicollinearity. Hierarchical Cluster Analysis (HCA) helps identify uncorrelated landscape descriptors without requiring a priori decisions about which metrics to include or exclude. Figure 3 shows a dendrogram depicting the hierarchical clustering of GI characteristics. The variables were grouped via a distance-based method to find fundamental structural links. Metrics with comparable spatial patterns have been shown to cluster at reduced linkage distances, as demonstrated with CA and PLAND, as well as ENN_MN (Euclidean Nearest Neighbour Mean Distance) and CLUMPY, which form compact clusters. As the distance between clusters grows, they gradually merge, which shows that measure groups are less alike overall. It has been observed that highly correlated clusters contain CA–PLAND, TE-ED and NP-PD. A relatively mid-level correlated cluster contains ENN_MN-CLUMPY and SH_MN-{LSI-(TE-ED)} as shown in dendrogram Figure 3.

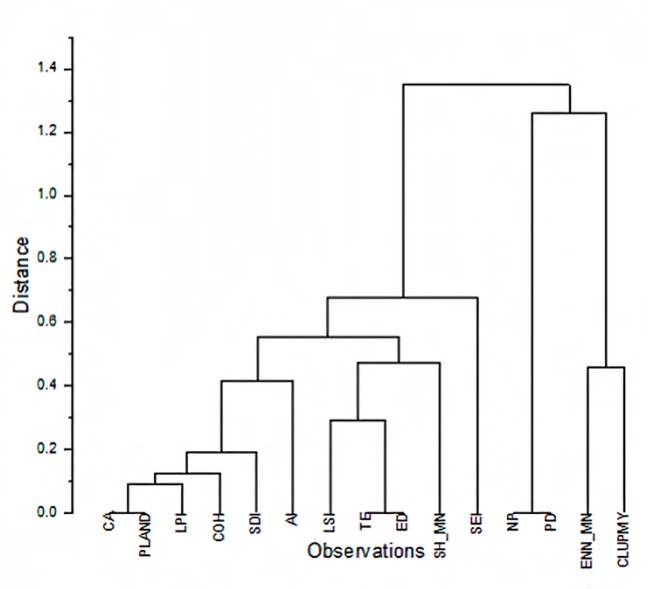

Figure 3. HCA of Green Infrastructure Landscape metrics

Seasonal Differences in Particulate Matter (PM) Pollution

The findings of an analysis of variance (ANOVA) revealed that there were significant differences ($p < 0.05$) between the PM10/2.5 concentrations during four distinct seasons. Both PM2.5 and PM10 concentrations were at their highest during the winter season, whereas both PM2.5 and PM10 concentrations were at their lowest level during the summer. It was discovered that the PM10/2.5 concentration in autumn was much higher than what was recorded in the spring. Possible reasons for significant fluctuations during the four seasons may include variations in air temperatures, humidity levels, wind direction and speed, presence or absence of leaves on vegetation, and patterns of fossil energy consumption. The winter season in Delhi is characterised by elevated pollution levels, which can be attributed to a combination of factors such as low temperatures, elevated humidity, and stagnant airflow. The circumstances are conducive to the trapping of pollutants in the atmosphere. In addition, the practice of burning agricultural residue in neighbouring states significantly contributes to the increased levels of pollution in Delhi during the winter months, as the area falls within the same boundary level airshed.

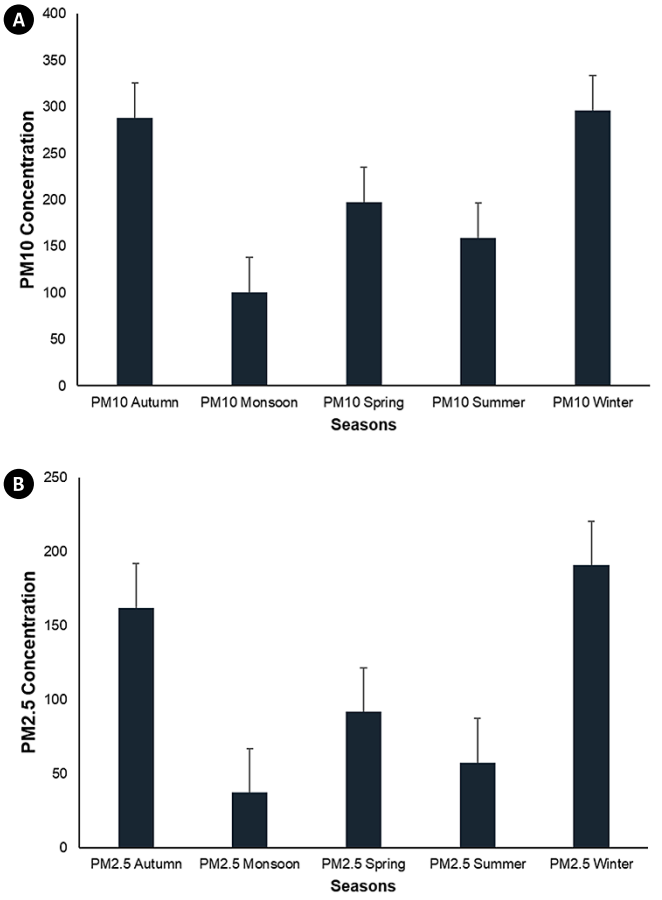

Figure 4. Analysis of variance (ANOVA) of PM2.5 and PM10 concentrations in four seasons. (A) seasonal ANOVA of PM10 concentration; (B) seasonal ANOVA of PM2.5 concentration

Principal Component Analysis (PCA)

Using PCA, we simplify the GI landscape-characterised data set by lowering its dimension. First, the predictor (response) variables (including PM2.5/10 value) and GI land-

scape characterise value defined as explanatory variables employed a centralised and standardised transformation, respectively. Then, the predictor variables are transformed into an equal number of principal components (PCs) to obtain a small number of components that could explain most (approximately 60%–90%) of the total variation in the predictor variables (Singh et al., 2013b; Wu et al., 2018). The percentage explained of variance and the cumulative proportion of variance are measures of the extent to which variation in PM pollution can be attributed to the presence of respective GI landscape characteristics along the first two principal component analysis (PCA) axes. The eigenvalues represent data variance along the principal component axis. The significant component with the highest eigenvalue explains the most data variation. In a PCA analysis, eigenvalues decide how many principal components must be retained. PCA explained 0.8204, 0.8626, 0.8668, 0.8429 and 0.8609 of the total variation in PM2.5, from scale 0.5 to scale 2.5. In contrast, the same axes explained 0.8377, 0.8392, 0.8477, 0.8518 and 0.8609 of the total variances in PM10 (Table. 3). Which suggested that the first two axes of PCA explain 82% to 86% of the variation for PM2.5 and 83% to 87% for PM10 with all the explanatory variables. Table 4. F-Ratio was used to test whether the multiscale GI characteristics affect PM pollution significantly, and R^2 represents the significance of PCA regression for the first seven PC axes, which explain more than 90% variance of PM pollution by GI characteristics in the PCA model, and the R^2adj was the adjusted or real value of the explained proportion. R^2 of PM2.5 from scale 0.5 km to scale 2.5 km were 0.9164, 0.9434, 0.8609, 0.9645, 0.9316, and R^2 of PM10 0.9502, 0.9287, 0.9717, 0.8566, 0.9753 respectively (Table 4). The tests indicated that landscape metrics of GI at all scales significantly explained the total variance of PM2.5 and PM10. Each scale included all the fifteen GI characterise metrics: CA, PLAND, SHAPE_MN, LSI, TE, COHESION, LPI, NP, PD, CLUMPY, ENN_MN, AI, SDI, ED, SEI. Positive and negative correlations with PCA axes indicate the direction and magnitude of the association between the features and the variables. By interpreting the PCA coefficients, we can gain insight into the underlying structure of the data and the relationships between the variables. The correlation between GI characteristics and the top two PCA axes of both PM2.5 and PM10 at a scale of 0.5 km × 0.5 km to 2.5 km × 2.5 km has been shown in Table 5. We selected the scales at which correlations between the PCA axes and PM concentration were significant based on the correlation that existed between the landscape metrics and the PCA axes seasonally.

PM2.5, CA (negative), PLAND (negative), TE (negative), and ED (negative) related to the first axis at all scales with minimal variation in the correlation coefficient, whereas all these GI characteristics showed relatively high negative relation at 0.5 to 1.5 km scale. NP (positive) and PD (positive) are significantly related to the first axis at all scales, whereas these are negatively related to PM2.5 at 2 km and 2.5 km. LPI (negative) and LSI (negative) were on a 1 km and 2.5 km scale, respectively. SH_MN (positive), ENN_MN (positive) and CLUMPY (positive) at 1.5 km scale with the second axis, 2.5 km scale with the first axis and 0.5 km scale with the first axis, respectively. COH (negative) at 2 km was significantly related to the second axis, whereas AI (positive) was significantly related at 0.5 km scale with the first axis. SDI (negative) and SEI (negative) with first and second axes, respectively, at 0.5 km and 1 km with first and second axes, respectively.

Table 3. PCA of PM2.5PM2.5 and PM10PM10 concentration on multiscale plots

Scale	Parameters	PCA1-PM2.5	PCA2-PM2.5	PCA1-PM10	PCA2-PM10
0.5	Eigenvalues	5.528	2.774	5.567	2.895
	Proportion explained of variance	0.618	0.307	0.609	0.322
	Cumulative proportion of variance	0.618	0.820	0.609	0.838
1	Eigenvalues	5.413	2.549	5.375	2.536
	Proportion explained of variance	0.595	0.283	0.590	0.284
	Cumulative proportion of variance	0.595	0.862	0.590	0.839
1.5	Eigenvalues	5.685	2.268	5.531	2.202
	Proportion explained of variance	0.634	0.262	0.623	0.257
	Cumulative proportion of variance	0.634	0.866	0.622	0.847
2	Eigenvalues	5.385	3.052	5.549	3.048
	Proportion explained of variance	0.643	0.346	0.652	0.344
	Cumulative proportion of variance	0.643	0.842	0.652	0.851
2.5	Eigenvalues	4.834	2.499	4.871	2.370
	Proportion explained of variance	0.623	0.279	0.622	0.275
	Cumulative proportion of variance	0.623	0.860	0.622	0.860

PM10, CA (negative), PLAND (negative), TE (negative), and ED (negative) are related to the first axis at all scales, with minimal variation having relatively high negative significant relation at a lower scale that is from 0.5 km to 1.5 km. NP (positive) and PD (positive) are significantly related to the first axis at 0.5 km scale. LPI (negative) and LSI (positive) at 2.5 km with the second axis. SH_MN (negative) at 1.5 km, ENN_MN (positive) significant relation at 2.5 km, CLUMPY (positive) at 1 km with first axis. COH (negative) at 0.5 km is significantly related to the second axis, whereas AI (positive) is significantly related at 0.5 km scale with the first axis. SDI (negative) and SEI (negative) with first and second axes, respectively, at 0.5 km and 1.5 km with first and second axes, respectively.

Table 4. Significance Test at $p < 0.05^*$

Test of Significance of all Canonical Axes	F-Ratio	R^2	R^2adj
PM2.5-0.5	0.0261	0.9164	0.8997
PM2.5-1	0.0171	0.9434	0.9321
PM2.5-1.5	0.0462	0.8609	0.8330
PM2.5-2	0.0105	0.9645	0.9574
PM2.5-2.5	0.0210	0.9316	0.9179
PM10-0.5	0.0025	0.9502	0.9403
PM10-1	0.0038	0.9287	0.9144
PM10-1.5	0.0049	0.9717	0.9660
PM10-2	0.0478	0.8566	0.8279
PM10-2.5	0.0072	0.9753	0.9703

Table 5. Correlation between Green Infrastructure characterise metrics and Principal Component Analysis (PCA) axes of scale and PM2.5/10 and Graphical representation respectively, $p < 0.05^*$.

Axes	CA	PLAND	NP	PD	LPI	LSI	SH_MN	ENN_MN	CLUMPY	COH	AI	SDI	SEI	TE	ED
PCA1-PM2.5-0.5	-2.05	-2.05	3.35	3.36	-2.03	-0.81	-1.12	3.71	3.83	-1.86	2.93	-1.87	0.66	-2.02	-2.02
PCA2-PM2.5-0.5	-0.19	-0.19	-1.95	-1.94	0.44	-2.45	1.76	1.07	-0.39	0.30	1.34	-0.07	-1.98	-0.53	-0.53
PCA1-PM2.5-1	-1.92	-1.92	3.10	3.10	0.57	-0.43	-1.50	4.21	3.82	-1.43	2.63	-1.65	-0.78	-2.11	-2.11
PCA2-PM2.5-1	-0.01	-0.01	1.73	1.73	-2.17	-2.64	1.70	-0.56	-1.29	-1.93	-1.38	0.02	-2.99	-0.01	-0.01
PCA1-PM2.5-1.5	-2.08	-2.08	3.29	3.28	-2.03	-0.81	-1.35	4.16	3.39	1.04	-1.29	-1.82	0.50	-1.96	-1.96
PCA2-PM2.5-1.5	0.01	0.01	0.87	0.86	0.49	-2.76	1.91	-0.01	-0.68	-1.77	2.08	0.64	2.79	-0.33	-0.33
PCA1-PM2.5-2	-1.92	-1.92	3.13	3.14	-1.83	-0.28	-1.49	4.31	3.64	0.82	-0.59	-1.70	0.69	-1.88	-1.88
PCA2-PM2.5-2	0.32	0.32	-1.85	-1.85	0.00	-2.66	-0.96	0.49	-0.43	-2.00	2.53	0.73	2.00	0.14	0.14
PCA1-PM2.5-2.5	-1.92	-1.97	2.46	2.45	-2.02	-0.81	-0.81	4.46	2.98	-0.15	-0.60	-1.85	0.04	-1.94	-1.84
PCA2-PM2.5-2.5	0.44	0.38	-2.11	-2.11	0.21	-2.79	1.57	0.85	2.25	-1.71	2.43	-0.61	-1.52	-0.45	-0.45
Significant negative Relation	-2.08	-2.08	-2.11	-2.11	-2.17	-2.79	-1.50	-0.56	-1.29	-2.00	-1.38	-1.87	-2.99	-2.11	-2.11
Significant Positive Relation	0.44	0.38	3.35	3.36	0.57	-0.28	1.91	4.46	3.83	1.04	2.93	0.73	2.79	0.14	0.14

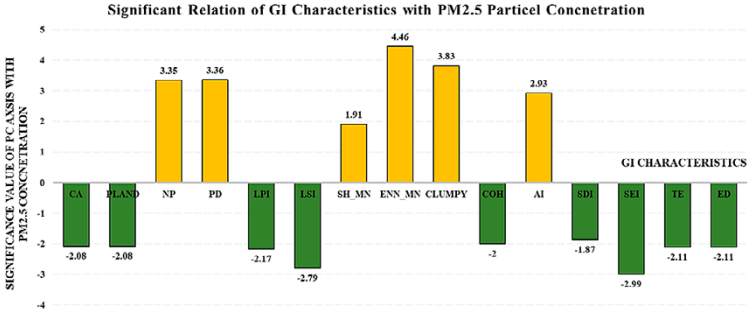

Axes	CA	PLAND	NP	PD	LPI	LSI	SH_MN	ENN_MN	CLUMPY	COH	AI	SDI	SEI	TE	ED
PCA1-PM10-0.5	-2.06	-2.06	3.22	3.22	-1.99	-0.01	-1.57	3.86	3.50	-0.29	2.92	-1.84	0.70	-2.05	-2.05
PCA2-PM10-0.5	-0.18	-0.18	2.36	2.35	-0.11	2.69	-1.58	-0.72	1.46	-2.33	1.46	-0.16	-1.84	-0.57	-0.57
PCA1-PM10-1	-1.89	-1.89	1.05	1.05	0.62	-0.40	-1.64	4.26	3.91	1.53	2.60	-1.63	-0.31	-2.06	-2.06
PCA2-PM10-1	-0.22	-0.22	3.08	3.08	-2.10	2.62	0.32	-0.20	-0.92	-1.72	-1.63	-0.40	-2.13	0.00	0.00
PCA1-PM10-1.5	-2.05	-2.04	3.21	3.21	-1.95	-0.58	-1.12	4.21	3.43	1.00	-1.07	-1.73	1.00	-2.00	-2.00
PCA2-PM10-1.5	-0.12	-0.12	1.17	1.16	-0.62	2.77	-2.14	0.02	-1.38	-1.80	-2.09	-0.69	-2.51	0.45	0.45
PCA1-PM10-2	-1.89	-1.89	3.07	3.08	-1.86	-0.73	-1.56	4.28	3.61	0.77	-0.19	-1.54	0.84	-1.96	-1.96
PCA2-PM10-2	-0.47	-0.46	-1.93	-1.93	-0.07	2.61	0.71	0.07	-0.55	-1.97	-2.51	-0.92	-1.73	0.75	0.75
PCA1-PM10-2.5	-2.00	-2.00	2.29	2.28	-2.11	-1.11	-0.93	4.44	3.66	-0.16	-0.29	-1.81	0.06	-1.94	-1.88
PCA2-PM10-2.5	0.77	0.76	2.37	2.37	0.21	2.17	-1.51	0.78	-1.26	-1.70	-2.34	-0.68	-1.66	0.70	0.69
Significant negative Relation	-2.06	-2.06	-1.93	-1.93	-2.11	-1.11	-2.14	-0.72	-1.38	-2.33	-2.51	-1.84	-2.51	-2.06	-2.06
Significant Positive Relation	0.77	0.76	3.22	3.22	0.62	2.77	0.71	4.44	3.91	1.53	2.92	-0.16	1.00	0.75	0.75

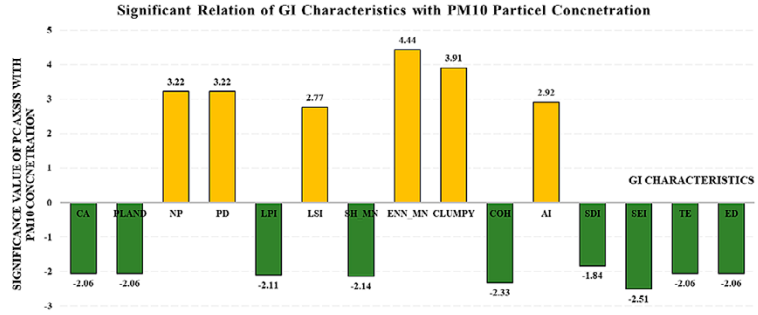

Discussion

In this study, we took PM pollution as the targeted urban environmental issue to be solved by the planning of GI. The study addresses the solution at the local level from 0.5 km to 2.5 km in alignment with the government approach of air quality management at the airshed level (Ganguly et al., 2020). The results provide the complex connections between GI design and PM pollution levels, as well as effective solutions for improving air quality via urban green space planning.

Season and scale-wise Effects of Green Infrastructure Characteristics on PM Pollution

ANOVA results revealed significant seasonal differences in PM concentrations, with the highest levels in winter and the lowest in summer. This variation is consistent with previous studies, which attribute winter pollution peaks to lower temperatures, stagnant air, higher humidity, and regional agricultural residue burning. PCA demonstrated that a considerable proportion of PM concentration variance (82%–87%) could be explained by the first two principal components, confirming the strong relationship between GI characteristics and air pollution. Scale sensitivity was evident, with smaller spatial scales (0.5–1.5 km) favoring compositional metrics like CA and PLAND since the vegetation cover serves as a sink for pollution (Liu et al., 2017; Zhang et al., 2021a) and promotes pollutant deposition (Hirabayashi et al., 2015; Hirabayashi et al., 2012; Tiwari & Kumar, 2020). At larger scales (2–2.5 km) configurational metrics such as LPI and ED favored, as the high ED zone of GI behaves as an air filter by creating a buffer or protective green boundary as the high ED zone of GI behaves as an air filter by creating a buffer or protective green boundary as the high ED zone of GI behaves as an air filter by creating a buffer or protective green boundary. These findings align with existing literature emphasizing that vegetative coverage impacts local air quality more directly at smaller scales, while spatial configuration plays a greater role at broader urban landscape levelsThe shape matrices of GI characteristics do not directly impact PM pollution reduction (Lei et al., 2018). High COH values in the landscape can be a tangible obstacle that intercepts and captures suspended particulate matter from the atmosphere (Li et al., 2021). The process of interception helps in the removal of particulate matter (PM) from the atmosphere, thereby leading to a reduction in its concentration. A high coefficient of COH supports the formation of microenvironments that facilitate the accumulation of settled dust, thereby mitigating its dispersion into the atmosphere (Ge et al., 2021). The spatial distribution of GI characteristics in a given area can impact the direction and flow of air movements across the terrain. The phenomenon of wind encountering an obstacle can result in a reduction of its velocity and a change in its direction, leading to the occurrence of turbulence. The phenomenon of turbulence helps in the dispersion and attenuation of particulate matter and other airborne pollutants by impeding their accumulation in specific regions. The process facilitates the amalgamation of uncontaminated air with contaminated air, decreasing the collective level of particulate matter (PM). AI significantly impacts PM10 reduction at higher scales of 1.5 km to 2.5 km. The findings were consistent with prior research, which suggested that the ability of urban green spaces to mitigate fine particulate matter was positively correlated with the proximity and contiguity of their landscape patches (Liu & Shen, 2014). Moreover, the escalating intricacy of the GI terrain typically amplifies the edge effects of GI landscapes, thereby aiding in the interception of particulate matter. SDI and SEI show significant reduction potential during summer at 0.5 km scale and during Autumn at 1.5 km. The SDI and SEI have the potential to demonstrate the heterogeneity of landscape patches, and their efficacy is based on the distribution of diverse patches. A higher index value indicates a landscape that is more evenly distributed. A higher degree of landscape distribution results in a stronger correlation between land use and increased interaction between “sink” and “source” landscapes, leading to a more frequent reduction of PM pollution (Łowicki, 2019). However, six configuration GI characteristics increase PM pollution during certain seasons at several scales.

Comparison of compositional and configurational GI on PM pollution variation

A comparative analysis revealed that compositional characteristics (e.g., CA, PLAND) are more effective in PM reduction at smaller spatial scales, where vegetation density directly contributes to pollutant deposition. On the other hand, configurational metrics (e.g., LPI, ED, COH, AI) played a stronger role at larger scales, influencing airflow patterns, turbulence, and pollutant dispersion. This reinforces the importance of a scale-sensitive GI design, as certain benefits—such as aerodynamic interactions and pollutant interception—become more pronounced with increasing spatial extent (Lei et al., 2018). The results also underscore the complex role of shape and spatial configuration metrics like LSI, SH_MN, COH, and AI. While high COH values were associated with PM reduction by forming barriers to airborne particulates, other metrics exhibited season-dependent or pollutant-specific effects. For instance, LSI showed a stronger association with PM2.5 reduction, while SH_MN was more relevant for PM10, highlighting the need for pollutant-specific GI design

strategies. The observed heterogeneity in GI–PM relationships across scales and seasons suggests that a one-size-fits-all approach to green space planning is insufficient. Instead, contextual design strategies are required. For example, denser vegetation patches (high CA/PLAND) should be prioritized in residential neighborhoods to improve local air quality, while connectivity and edge complexity (high ED/LPI/AI) should be enhanced in larger parks or peri-urban buffers to leverage wind interactions and pollutant dispersion.The presence of a greater number of trees within a street canyon may result in decreased ventilation and an overall rise in air pollution levels (Chen et al, 2018; Zhou et al., 2019). Additionally, studies have also shown that the existence of high-level vegetation canopies, such as trees, can lead to a decline in air quality. In contrast, low-level green infrastructure, such as hedges, can enhance air-quality conditions (Wu et al., 2018b; Hirabayashi et al., 2012; Srbinovska et al., 2021). The correlation between spatial configurations and PM concentration exhibited heterogeneity across various seasons and scales. Additionally, the landscape metrics of green space exhibited both positive and negative impacts on PM concentration. Therefore, the efficacy of green space in mitigating PM concentration is contingent upon the equilibrium between these advantages and disadvantages.

Limitation

This study increased our understanding of PM pollution and urban green space spatial patterns, but it had some constraints, though the following assumptions and conditions were adopted to try to minimise the constraints. Based on the conditions and assumptions, this study picked the most significant number of plots possible for the study. Future research may benefit from more sample plot data. The following criteria and presumptions were used to choose monitoring stations for study: (i) Major modifiers like substantial bodies of water are absent from AOI; (ii) Data on PM concentrations on rainy days were excluded from the research; (iii) Monitoring stations were located in certain local climatic zones (LCZs) so as to have the least amount of disagreement owing to built-up morphology in the research. Interpolated PM concentration map data was used to calculate each plot's PM concentration value, which was verified statistically, and the mean value was estimated at each scale. In future studies, more monitoring stations may be used to achieve a more accurate concentration value. High-resolution geospatial data may help map green infrastructure landscape patterns more accurately. The association between PM pollution and greenspace patterns must be examined with respect to wind speed and direction. Other weather-related characteristics are also required.

Conclusion

The relationship between PM pollution and the greenspace pattern was not as straightforward as anticipated. In this study, we took Delhi as an example, one of the most polluted cities in India.This study provides a comprehensive multiscale and seasonal assessment of the influence of GI landscape characteristics on particulate matter (PM2.5 and PM10) pollution in an urban context. Key findings indicate that compositional metrics such as CA and PLAND consistently show strong negative correlations with PM concentrations across all seasons and spatial scales, underscoring the role of vegetation cover in pollutant deposition. Similarly, TE and ED metrics contribute significantly to PM reduction, particularly during the autumn and winter months at lower scales, by enhancing the buffering capacity of green spaces. Configurational metrics such as LPI, LSI, and COH also exhibited scale- and season-specific effectiveness. Their influence on PM pollution was more pronounced at larger spatial scales, highlighting the importance of spatial arrangement and connectivity of GI patches. The study also emphasizes the dual role of GI: while certain configurations reduce PM through improved dispersion and deposition, others—especially dense, high-canopy vegetation in confined spaces—may hinder air circulation and increase PM accumulation. This reinforces the need for context-specific GI design strategies that balance aerodynamic and deposition effects for optimal air quality outcomes. The research perfectly aligns with the government's strategy for reducing air pollution by focusing on airsheds. Overall, the findings provide actionable insights for urban planners and policymakers. By tailoring GI interventions to scale, configuration, and seasonal dynamics, cities can enhance the effectiveness of green infrastructure as a nature-based solution for urban air quality management. Future research incorporating more monitoring stations, high-resolution spatial data, and additional meteorological variables will further refine the understanding of GI–PM dynamics.

Acknowledgements

The authors sincerely thank the Indian Institute of Technology Roorkee for providing the necessary facilities and assistance for this study. The authors express gratitude to the Central Pollution Control Board (CPCB) for providing access to the air quality data used in this study. The authors express gratitude for the support and motivation from colleagues and mentors, whose advice significantly enhanced our study.

References

Agarwal, M., & Tandon, A. (2010). Modeling of the urban heat island in the form of mesoscale wind and of its effect on air pollution dispersal. *Applied Mathematical Modelling*, 34(9), 2520–2530. https://doi.org/10.1016/j.apm.2009.11.016

Ahern, J. (2007). Green infrastructure for cities: The spatial dimension. In *Cities ofthe Future Towards Integrated Sustainable Water and Landscape Management* (pp. 267–283). http://citeseerx.ist.psu.edu/viewdoc/download;jsessionid=E549A4EF0DF3B927AD82A5B40BA1C2B1?doi=10.1.1.558.8386&rep=rep1&type=pdf

AlKhaled, S., Coseo, P., Brazel, A., Cheng, C., & Sailor, D. (2020). Between aspiration and actuality: A systematic review of morphological heat mitigation strategies in hot urban deserts. *Urban Climate*, 31, 100570. https://doi.org/10.1016/j.uclim.2019.100570

Andersson-Sköld, Y., Klingberg, J., Gunnarsson, B., Cullinane, K., Gustafsson, I., Hedblom, M., Knez, I., Lindberg, F., Ode Sang, Å., Pleijel, H., Thorsson, P., & Thorsson, S. (2018). A framework for assessing urban greenery's effects and valuing its ecosystem services. *Journal of Environmental Management*, 205, 274–285. https://doi.org/10.1016/j.jenvman.2017.09.071

Andrew, S. M., Moe, S. R., Totland, Ø., & Munishi, P. K. T. (2012). Species composition and functional structure of herbaceous vegetation in a tropical wetland system. *Biodiversity and Conservation*, 21(11), 2865–2885. https://doi.org/10.1007/s10531-012-0342-y

Ashok, A., Rani, H. P., & Jayakumar, K. V. (2021). Monitoring of dynamic wetland changes using NDVI and NDWI based landsat imagery. *Remote Sensing Applications: Society and Environment*, 23, 100547. https://doi.org/10.1016/j.rsase.2021.100547

Banerjee, T., Murari, V., Kumar, M., & Raju, M. P. (2015). Source apportionment of airborne particulates through receptor modeling: Indian scenario. *Atmospheric Research*, 164–165, 167–187. https://doi.org/10.1016/j.atmosres.2015.04.017

Bartesaghi-Koc, C., Osmond, P., & Peters, A. (2019). Mapping and classifying green infrastructure typologies for climate-related studies based on remote sensing data. *Urban Forestry and Urban Greening*, 37(July 2017), 154–167. https://doi.org/10.1016/j.ufug.2018.11.008

Bartesaghi Koc, C., Osmond, P., & Peters, A. (2018). Evaluating the cooling effects of green infrastructure: A systematic review of methods, indicators and data sources. *Solar Energy*, 166(April), 486–508. https://doi.org/10.1016/j.solener.2018.03.008

Barwise, E. Y. (2023). *Developing a design framework for enhanced air pollution mitigation by urban green infrastructure* [University of Surrey Guildford, Surrey, GU2 7XH, United Kingdom]. https://openresearch.surrey.ac.uk/esploro/outputs/doctoral/Developing-a-design-framework-for-enhanced/99890066602346

Benedict, M. A., McMahon, E., & Conservation Fund (Arlington, V. . (2006). *Green infrastructure : linking landscapes and communities*. Island Press.

Bezyk, Y., Sówka, I., Górka, M., & Blachowski, J. (2021). Gis-based approach to spatio-temporal interpolation of atmospheric co2 concentrations in limited monitoring dataset. *Atmosphere*, 12(3), 1–25. https://doi.org/10.3390/atmos12030384

Calfapietra, C., & Cherubini, L. (2019). Green Infrastructure: Nature-Based Solutions for sustainable and resilient cities. *Urban Forestry and Urban Greening*, 37, 1–2. https://doi.org/10.1016/J.UFUG.2018.09.012

Cao, W., Zhou, W., Yu, W., & Wu, T. (2024). Combined effects of urban forests on land surface temperature and PM2.5 pollution in the winter and summer. *Sustainable Cities and Society*, 104(February), 105309. https://doi.org/10.1016/j.scs.2024.105309

Central Pollution Control Board. (2003). Guidelines for Ambient Air Quality Monitoring. *National Ambient Air Quality Monitoring, NAAQMS*, 2003–2004. https://doi.org/10.1080/15265160903581718

Chatterji, A. (2020). Air Pollution in Delhi: Filling the Policy Gaps. *Observer Research Foundation, December*. https://www.orfonline.org/research/air-pollution-delhi-filling-policy-gaps/

Chelani, A. B., Gajghate, D. G., Tamhane, S. M., & Hasan, M. Z. (2001). Statistical modeling of ambient air pollutants in Delhi. *Water, Air, and Soil Pollution*, 132(3–4), 315–331. https://doi.org/10.1023/A:1013204120867

Chen, M., & Dai, F. (2022). PCA-Based Identification of Built Environment Factors Reducing PM2.5 Pollution in Neighborhoods of Five Chinese Megacities. *Atmosphere*, 13(1). https://doi.org/10.3390/atmos13010115

Chen, M., Dai, F., Yang, B., & Zhu, S. (2019). Effects of neighborhood green space on PM 2 . 5 mitigation : Evidence from five megacities in China. *Building and Environment*, 156(March), 33–45. https://doi.org/10.1016/j.buildenv.2019.03.007

Chen, M., Dai, F., & Zhu, S. (2018). Effects of spatial forms of green infrastructure in block scale on PM10 and PM2.5 removal - A case study of the main city of Wuhan. *Landscape Research Record*, 7.

CleanAirAsia. (2016). *Guidance Framework for Better Air Quality in Asian Cities*.

CPCB. (2013). News Letter CPCB. *Cpcbenvis*, 53(9), 1689–1699.

CPCB. (2015). *CPCB Data Protocol*.

Dhingra, C. (2020). *Assessment of AIR Quality Index for Delhi region_* A comparison between odd-even policy 2019 and Lock Down Period.

Dissanayake, D., Morimoto, T., & Murayama, Y. (2018). Impact of Urban Surface Characteristics and Socio-Economic Variables on the Spatial Variation of Land Surface Temperature in Lagos City, Nigeria. *Sustainability*, 11(25). https://doi.org/10.3390/su11010025

Elhaik, E. (2022). Principal Component Analyses (PCA)-based findings in population genetic studies are highly biased and must be reevaluated. In *Scientific Reports* (Vol. 12, Issue 1). Nature Publishing Group UK. https://doi.org/10.1038/s41598-022-14395-4

Fan, C., Myint, S. W., & Zheng, B. (2015). Measuring the spatial arrangement of urban vegetation and its impacts on seasonal surface temperatures. *Progress in Physical Geography*, 39(2), 199–219. https://doi.org/10.1177/0309133314567583

Forman, R. T. T. (1995). *Some general principles of landscape and regional ecology*. 10(3), 133–142.

Franklin, S. B., Gibson, D. J., Robertson, P. A., Pohlmann, J. T., Fralish, J. S., Scott, B., David, J., Philip, A., John, T., & James, S. (1995). Parallel Analysis : a Method for Determining Significant Principal Components significant principal components. *Journal of Vegetation Scienc*, 6(1), 99–106.

Ganguly, T., Selvaraj, K. L., & Guttikunda, S. K. (2020). National Clean Air Programme (NCAP) for Indian cities: Review and outlook of clean air action plans. *Atmospheric Environment*: X, 8, 100096. https://doi.org/10.1016/j.aeaoa.2020.100096

Gašparović, M., & Dobrinić, D. (2021). Green infrastructure mapping in urban areas using sentinel-1 imagery. *Croatian Journal of Forest Engineering*, 42(2), 337–356. https://doi.org/10.5552/crojfe.2021.859

Ge, M., Fang, S., Gong, Y., Tao, P., Yang, G., & Gong, W. (2021). Understanding the Correlation between Landscape Pattern and Vertical Urban Volume by Time-Series Remote Sensing Data: A Case Study of Melbourne. *ISPRS International Journal of Geo-Information*, 10(1), 14. https://doi.org/10.3390/ijgi10010014

Ginevan, M. E., & Splistone, D. E. (2004). Statistical Tools for Environemntal Quality Measurement. In *Applied Environemntal Statistics* (Vol. 59).

Grafius, D. R., Corstanje, R., & Harris, J. A. (2018). Linking ecosystem services, urban form and green space configuration using multivariate landscape metric analysis. *Landscape Ecology*, 33(4), 557–573. https://doi.org/10.1007/s10980-018-0618-z

Greenpeace. (2020). Toxiz Air: The Price of Fossil Fules (Issue February).

Grimm, N. B., Faeth, S. H., Golubiewski, N. E., Redman, C. L., Wu, J., Bai, X., & Briggs, J. M. (2008). Global Change and the Ecology of Cities. *Science*, 319(February).

Grover, A., & Singh, R. B. (2015). Analysis of urban heat island (UHI) in relation to normalized difference vegetation index (NDVI): A comparative study of delhi and mumbai. *Environments - MDPI*, 2(2), 125–138. https://doi.org/10.3390/environments2020125

Gulia, S., Shiva Nagendra, S. M., Khare, M., & Khanna, I. (2015a). Urban air quality management-A review. *Atmospheric Pollution Research*, 6(2), 286–304. https://doi.org/10.5094/APR.2015.033

Gulia, S., Shiva Nagendra, S. M., Khare, M., & Khanna, I. (2015b). Urban air quality management-A review. *Atmospheric Pollution Research*, 6(2), 286–304. https://doi.org/10.5094/APR.2015.033

Guo, G., Wu, Z., Cao, Z., Chen, Y., & Zheng, Z. (2021). Location of greenspace matters: a new approach to investigating the effect of the greenspace spatial pattern on urban heat environment. *Landscape Ecology*, 0123456789. https://doi.org/10.1007/s10980-021-01230-w

Gupta, U. (2008). Valuation of urban air pollution: A case study of Kanpur City in India. In *Environmental and Resource Economics* (Vol. 41, Issue 3). https://doi.org/10.1007/s10640-008-9193-0

Guttikunda, S. K., & Calori, G. (2013). A GIS based emissions inventory at 1 km × 1 km spatial resolution for air pollution analysis in Delhi, India. *Atmospheric Environment*, 67, 101–111. https://doi.org/10.1016/j.atmosenv.2012.10.040

Guttikunda, S. K., Goel, R., & Pant, P. (2014). Nature of air pollution, emission sources, and management in the Indian cities. *Atmospheric Environment*, 95, 501–510. https://doi.org/10.1016/j.atmosenv.2014.07.006

Guttikunda, S. K., Nishadh, K. A., & Jawahar, P. (2019). Air pollution knowledge assessments (APnA) for 20 Indian cities. *Urban Climate*, 27(November 2018), 124–141. https://doi.org/10.1016/j.uclim.2018.11.005

Heo, S., Bell, M. L., Haven, N., & States, U. (2020). The Influence of Green Space on the Short-term Effects of Particulate Matter on Hospitalization in the U.S. for

2000–2013. *Environment Research*, 174, 61–68. https://doi.org/10.1016/j.envres.2019.04.019

Hirabayashi, S., Kroll, C. N., & Nowak, D. J. (2012). Development of a distributed air pollutant dry deposition modeling framework. *Environmental Pollution*, 171, 9–17. https://doi.org/10.1016/j.envpol.2012.07.002

Hirabayashi, S., Kroll, C. N., & Nowak, D. J. (2015). *i-Tree Eco Dry Deposition Model Descriptions*. http://www.itreetools.org/eco/resources/iTree_Eco_Dry_Deposition_Model_Descriptions.pdf

Hofman, J., Bartholomeus, H., Janssen, S., Calders, K., Wuyts, K., Van Wittenberghe, S., & Samson, R. (2016). Influence of tree crown characteristics on the local PM10 distribution inside an urban street canyon in Antwerp (Belgium): A model and experimental approach. *Urban Forestry and Urban Greening*, 20(2016), 265–276. https://doi.org/10.1016/j.ufug.2016.09.013

Im, J. (2019). Green streets to serve urban sustainability: Benefits and typology. *Sustainability (Switzerland)*, 11(22). https://doi.org/10.3390/su11226483

Impacts, E. (n.d.). *AIR*.

IQAir. (2021). *World Air Qualtiy Report*.

Irga, P. J., Burchett, M. D., & Torpy, F. R. (2015). Does urban forestry have a quantitative effect on ambient air quality in an urban environment? *Atmospheric Environment*, 120, 173–181. https://doi.org/10.1016/j.atmosenv.2015.08.050

Jain, D., Bhatnagar, S., Rathi, V., Sharma, D., & Sachdeva, K. (2021). Mainstreaming Built Environment for Air Pollution Management Plan in Delhi. *Economic and Political Weekly*, 2019, 19–22. https://www.epw.in/journal/2021/6/commentary/mainstreaming-built-environment-air-pollution.html%0Ahttps://www.epw.in/system/files/pdf/2021_56/5/CM_LVI_06_060221_DeeptyJain_6Feb2021_Pages 19-22.pdf

Jalan, I. (2019). *What is Polluting Delhi ' s Air ? Understanding Uncertainties in Emissions Inventories* (Issue March).

Jeanjean, A., Buccolieri, R., Eddy, J., Monks, P., & Leigh, R. (2017). Air quality affected by trees in real street canyons: The case of Marylebone neighbourhood in central London. *Urban Forestry and Urban Greening*, 22, 41–53. https://doi.org/10.1016/j.ufug.2017.01.009

Jeanjean, A. P. R., Monks, P. S., & Leigh, R. J. (2016). Modelling the effectiveness of urban trees and grass on PM2.5 reduction via dispersion and deposition at a city scale. *Atmospheric Environment*, 147, 1–10. https://doi.org/10.1016/j.atmosenv.2016.09.033

Jiang, L., & O'Neill, B. C. (2017). Global urbanization projections for the Shared Socioeconomic Pathways. *Global Environmental Change*, 42, 193–199. https://doi.org/10.1016/j.gloenvcha.2015.03.008

Jiang, R., Xie, C., Man, Z., Afshari, A., & Che, S. (2023). LCZ method is more effective than traditional LUCC method in interpreting the relationship between urban landscape and atmospheric particles. *Science of the Total Environment*, 869(October 2022), 161677. https://doi.org/10.1016/j.scitotenv.2023.161677

Jolliffe, I. T., Cadima, J., & Cadima, J. (2016). Principal component analysis : a review and recent developments Subject Areas. *The Royal Society*, 374.

Kenkel, N. C. (2006). On selecting an appropriate multivariate analysis. *Canadian Journal of Plant Science*, 86(3), 663–676. https://doi.org/10.4141/P05-164

Kotharkar, R., & Bagade, A. (2018). Evaluating urban heat island in the critical local climate zones of an Indian city. *Landscape and Urban Planning*, 169, 92–104. https://doi.org/10.1016/J.LANDURBPLAN.2017.08.009

Kumar, P., Abhijith, K. V., & Barwise, Y. (2019). *Implementing Green Infrastructure for Air Pollution Abatement: General Recommendations for Management and Plant Species Selection. August*. https://doi.org/doi.org/10.6084/m9.figshare.8198261.v1

Kumar, P., Druckman, A., Gallagher, J., Gatersleben, B., Allison, S., Eisenman, T. S., Hoang, U., Hama, S., Tiwari, A., Sharma, A., Abhijith, K. V., Adlakha, D., McNabola, A., Astell-Burt, T., Feng, X., Skeldon, A. C., de Lusignan, S., & Morawska, L. (2019). The nexus between air pollution, green infrastructure and human health. *Environment International*, 133(September). https://doi.org/10.1016/j.envint.2019.105181

Kushwaha, S., & Nithiyanandam, Y. (2019). The study of heat island and its relation with urbanization in Gurugram, Delhi NCR for the period of 1990 to 2018. *International Archives of the Photogrammetry, Remote Sensing and Spatial Information Sciences - ISPRS Archives*, 42(5/W3), 49–56. https://doi.org/10.5194/isprs-archives-XLII-5-W3-49-2019

Lavigne, E., Yasseen, A. S., Stieb, D. M., Hystad, P., Donkelaar, A. Van, Martin, R. V, Brook, J. R., Crouse, D. L., Burnett, R. T., Chen, H., Weichenthal, S., Johnson, M., Villeneuve, P. J., & Walker, M. (2016). Ambient air pollution and adverse birth outcomes : Differences by maternal comorbidities. *Environmental Research*, 148, 457–466. https://doi.org/10.1016/j.envres.2016.04.026

Leão, M. L. P., Zhang, L., & da Silva Júnior, F. M. R. (2023). Effect of particulate matter (PM2.5 and PM10) on health indicators: climate change scenarios in a Brazilian metropolis. *Environmental Geochemistry and Health*, 45(5), 2229–2240. https://doi.org/10.1007/s10653-022-01331-8

Lei, Y., Davies, G. M., Jin, H., Tian, G., & Kim, G. (2021). Scale-dependent effects of urban greenspace on particulate matter air pollution. *Urban Forestry & Urban Greening*, 61(March), 127089. https://doi.org/10.1016/j.ufug.2021.127089

Lei, Y., Duan, Y., He, D., Zhang, X., Chen, L., Li, Y., Gao, Y. G., Tian, G., & Zheng, J. (2018). Effects of urban greenspace patterns on particulate matter pollution in metropolitan Zhengzhou in Henan, China. *Atmosphere*, 9(5), 1–15. https://doi.org/10.3390/ATMOS9050199

Li, K., Li, C., Liu, M., Hu, Y., Wang, H., & Wu, W. (2021). Multiscale analysis of the effects of urban green infrastructure landscape patterns on PM2.5 concentrations in an area of rapid urbanization. *Journal of Cleaner Production*, 325(October), 129324. https://doi.org/10.1016/j.jclepro.2021.129324

Li, X. (2017). Air Pollution: a global Problem Needs local Fixes. *Springer Nature*, 5, 9–11.

Li, X., Zhou, W., & Ouyang, Z. (2013). Relationship between land surface temperature and spatial pattern of greenspace: What are the effects of spatial resolution? *Landscape and Urban Planning*, 114, 1–8. https://doi.org/10.1016/j.landurbplan.2013.02.005

Li, Y. (2016). A Review of Air Pollution Control Policy Development and Effectiveness in China. *Intech*, *i*(tourism), 13.

Liang, L., & Gong, P. (2020). Urban and air pollution: a multi-city study of long-term effects of urban landscape patterns on air quality trends. *Scientific Reports*, 10(1), 1–13. https://doi.org/10.1038/s41598-020-74524-9

Liu, H., & Shen, Y. (2014). *The Impact of Green Space Changes on Air Pollution and Microclimates: A Case Study of the Taipei Metropolitan Area*. 8827–8855. https://doi.org/10.3390/su6128827

Liu, Y., Wu, J., & Yu, D. (2017). Characterizing spatiotemporal patterns of air pollution in China: A multiscale landscape approach. *Ecological Indicators*, 76, 344–356. https://doi.org/10.1016/j.ecolind.2017.01.027

Londoño-Ciro, L. A., & Cañón-Barriga, J. E. (2015). Imputation of spatial air quality data using gis-spline and the index of agreement in sparse urban monitoring networks. In *Revista Facultad de Ingenieria*, 76, 73–81. https://doi.org/10.17533/udea.redin.n76a09

Łowicki, D. (2019). Landscape pattern as an indicator of urban air pollution of particulate matter in Poland. *Ecological Indicators*, 97(September 2018), 17–24. https://doi.org/10.1016/j.ecolind.2018.09.050

Luo, H., Han, Y., Cheng, X., Lu, C., & Wu, Y. (2020). Spatiotemporal Variations in Particulate Matter and Air Quality over China: National, Regional and Urban Scales. *Atmosphere*, 12(1), 43. https://doi.org/10.3390/atmos12010043

Mannucci, P. M., Harari, S., Martinelli, I., & Franchini, M. (2015). Effects on health of air pollution: a narrative review. *Internal and Emergency Medicine*, 10(6), 657–662. https://doi.org/10.1007/s11739-015-1276-7

Mathers, C., Vos, T., & Stevenson, C. (1999). *The burden of disease and injury in Australia* (pp. 216–222).

Mcdonald, A. G., Bealey, W. J., Fowler, D., Dragosits, U., Skiba, U., Smith, R. I., Donovan, R. G., Brett, H. E., Hewitt, C. N., & Nemitz, E. (2007). *Quantifying the effect of urban tree planting on concentrations and depositions of PM 10 in two UK conurbations*. 41, 8455–8467. https://doi.org/10.1016/j.atmosenv.2007.07.025

Mcgarigal, K. (2015). Fragstats. *Fragstats*, April, 1–182.

McGarigal, K. (1995). *FRAGSTATS : Spatial Pattern Analysis Program for Quantifying Landscape Structure*. *August*.

McGarigal, K., Cushman, S. A., Neel, M. C., & Ene, E. (2002). *FRAGSTATS: spatial pattern analysis program for categorical maps* [internet].[cited 2009 October 12]. January 2002.

Meng, F., Tang, W., Gao, J., Ma, T., Li, Y., Du, X., Liu, J., Yang, Y., & Yu, Y. (2025). A Receptor Model and CTM Integrated PM2.5 Source Apportionment Approach and Its Application in 2 + 26 Cities Region of China Apportionment Approach and Its Application in 2 + 26 Cities Region of China. *Atmospheric Science and Meteorology*, 0–15. https://doi.org/10.20944/preprints202503.2207.v1

Menon, J. S., & Sharma, R. (2021). Nature-Based Solutions for Co-mitigation of Air Pollution and Urban Heat in Indian Cities. *Frontiers in Sustainable Cities*, 3(October), 1–11. https://doi.org/10.3389/frsc.2021.705185

Ministry Of Environment & Forests. (1987). *Air pollution control areas in various ut (s)* (Issue February, p. 14012).

Molina, M. J., Molina, L. T., Molina, M. J., & Molina, L. T. (2012). *Megacities and Atmospheric Pollution Megacities and Atmospheric Pollution*. 2247(2004). https://doi.org/10.1080/10473289.2004.10470936

Morelli, X., Rieux, C., Cyrys, J., Forsberg, B., & Slama, R. (2016). *Air pollution , health and social deprivation : A fine-scale risk assessment*. 147, 59–70. https://doi.org/10.1016/j.envres.2016.01.030

Myint, S. W., Zheng, B., Talen, E., Fan, C., Kaplan, S., Middel, A., Smith, M., Huang, H. ping, & Brazel, A. (2015). Does the spatial arrangement of urban landscape matter? examples of urban warming and cooling in phoenix and las vegas. *Ecosystem Health and Sustainability*, 1(4), 1–15. https://doi.org/10.1890/EHS14-0028.1

Nations, U., Programme, E., This, R., United, T., Environment, N., Nations, U., Programme, E., The, D., Nations, U., Programme, E., Nations, U., Programme, E., Nations, U., Programme, E., Nations, U., Programme, E., Pollution, A., This, S. S., Pacific, A., … Coalition, C. A. (2018). Air Pollution in Asia and the Pacific: Science-based solutions. In *United Nations Environment Programme*. http://www.ccacoalition.org/en/resources/air-pollution-asia-and-pacific-science-based-solutions

Nautiyal, S. N., Joshi, V., Gautam, A. S., Kumar, R., Kumar, S., Singh, K., & Gautam, S. (2025). Characterization and source apportionment of PM2.5 and PM10 in a Mountain Valley: seasonal variations, morphology, and elemental composition. *Journal of Atmospheric Chemistry*, 82(1). https://doi.org/10.1007/s10874-025-09469-2

Nowak, D. J., Crane, D. E., & Stevens, J. C. (2006). Air pollution removal by urban trees and shrubs in the United States. *Urban Forestry and Urban Greening*, 4(3–4), 115–123. https://doi.org/10.1016/j.ufug.2006.01.007

NWGITT. (2008). *Green Infrastructure Guide*.

Ou, Y., Rousseau, A. N., Wang, L., & Yan, B. (2017). Spatio-temporal patterns of soil organic carbon and pH in relation to environmental factors—A case study of the Black Soil Region of Northeastern China. *Agriculture, Ecosystems and Environment*, 245(May), 22–31. https://doi.org/10.1016/j.agee.2017.05.003

Ouyang, W., Morakinyo, T. E., Ren, C., Liu, S., & Ng, E. (2021). Thermal-irradiant performance of green infrastructure typologies: Field measurement study in a subtropical climate city. *Science of the Total Environment*, 764, 144635. https://doi.org/10.1016/j.scitotenv.2020.144635

Peters, A. (2011). Ambient Particulate Matter and the Risk for Cardiovascular Disease. *Progress in Cardiovascular Diseases*, 53, 327–333. https://doi.org/10.1016/j.pcad.2011.02.002

Power, A. L., Tennant, R. K., Stewart, A. G., Gosden, C., Worsley, A. T., Jones, R., & Love, J. (2023). The evolution of atmospheric particulate matter in an urban landscape since the Industrial Revolution. *Scientific Reports*, 13(1), 1–15. https://doi.org/10.1038/s41598-023-35679-3

Ramadan, B. S., Budihardjo, M. A., Syafrudin, Huboyo, H. S., & Sari, S. A. (2025). Analysis of particulate matter (PM10 and PM2.5) emissions from Jatibarang landfill: implications for air quality and health. *IOP Conference Series: Earth and Environmental Science*, 1477(1). https://doi.org/10.1088/1755-1315/1477/1/012033

Ramaiah, M., & Avtar, R. (2019). Urban Green Spaces and Their Need in Cities of Rapidly Urbanizing India: A Review. *Urban Science*, 3(3), 94. https://doi.org/10.3390/urbansci3030094

Ramani, P., Shah, C., Parikh, D., & Dadhaniya, B. (2019). Air pollution effect on urban areas. *Pramana Research Journal*, 9(9), 1–12.

Ramyar, R., & Zarghami, E. (2017). Green infrastructure contribution for climate change adaptation in urban landscape context. *Applied Ecology and Environmental Research*, 15(3), 1193–1209. https://doi.org/10.15666/aeer/1503_11931209

Rezaei, N., & Millard-Ball, A. (2023). Urban form and its impacts on air pollution and access to green space: A global analysis of 462 cities. *PLoS ONE*, 18(1 January), 1–26. https://doi.org/10.1371/journal.pone.0278265

Rohde, R. A., & Muller, R. A. (2015). Air Pollution in China : Mapping of Concentrations and Sources. *PLoS ONE*, 2, 1–14. https://doi.org/10.1371/journal.pone.0135749

Role, T. (2021). *Integrating Clean Air* , Climate , and Health Policies in the COVID-19 Era. March.

Sangkham, S., Phairuang, W., Sherchan, S. P., Pansakun, N., Munkong, N., Sarndhong, K., Islam, M. A., & Sakunkoo, P. (2024). An update on adverse health effects from exposure to PM2.5. *Environmental Advances*, 18(September), 100603. https://doi.org/10.1016/j.envadv.2024.100603

Saraswat, I., Mishra, R. K., & Kumar, A. (2017). Estimation of PM10 concentration from Landsat 8 OLI satellite imagery over Delhi, India. *Remote Sensing Applications: Society and Environment*, 8(April), 251–257. https://doi.org/10.1016/j.rsase.2017.10.006

Sathyakumar, V., Ramsankaran, R. A. A. J., & Bardhan, R. (2020). Geospatial approach for assessing spatiotemporal dynamics of urban green space distribution among neighbourhoods: A demonstration in Mumbai. *Urban Forestry and Urban Greening*, 48(December 2019), 126585. https://doi.org/10.1016/j.ufug.2020.126585

Schneekloth, L. H. (2000). Urban green infrastructure. In *Time-Saver Standards for Urban* Design (Issue 1987).

Selmi, W., Weber, C., Rivière, E., Blond, N., Mehdi, L., & Nowak, D. (2016). Air pollution removal by trees in public green spaces in Strasbourg city, France. *Urban Forestry and Urban Greening*, 17(2), 192–201. https://doi.org/10.1016/j.ufug.2016.04.010

Shareef, M. M., Husain, T., & Alharbi, B. (2016). Optimization of Air Quality Monitoring Network Using GIS Based Interpolation Techniques. *Journal of Environmental Protection*, 7(6), 895–911. https://doi.org/10.4236/jep.2016.76080

Sharma, S. K., Mandal, T. K., Saxena, M., Rashmi, Rohtash, Sharma, A., & Gautam, R. (2014). Source apportionment of PM10 by using positive matrix factorization at an urban site of Delhi, India. *Urban Climate*, 10, 656–670. https://doi.org/10.1016/j.uclim.2013.11.002

Singh, N., Singh, S., & Mall, R. K. (2020). Urban ecology and human health: implications of urban heat island, air pollution and climate change nexus. In *Urban Ecology*. Elsevier Inc. https://doi.org/10.1016/b978-0-12-820730-7.00017-3

Singh, P., & Tyagi, A. (2013a). Applying Kriging Approach on Pollution Data Using GIS Software. *International Journal of Environmental Engineering and Management*, 4(3), 185–190. http://www.ripublication.com/ijeem.htm

Singh, V., Guizani, N., Al-Alawi, A., Claereboudt, M., & Rahman, M. S. (2013b). Instrumental texture profile analysis (TPA) of date fruits as a function of its physico-chemical properties. *Industrial Crops and Products*, 50, 866–873. https://doi.org/10.1016/j.indcrop.2013.08.039

Sinnett, D., Smith, N., & Burgess, S. (2015). Handbook on green infrastructure: Planning, design and implementation. *Handbook on Green Infrastructure: Planning, Design and Implementation*, 1–474. https://doi.org/10.4337/9781783474004

Song, Z., Li, R., Qiu, R., Liu, S., Tan, C., Li, Q., Ge, W., Han, X., Tang, X., Shi, W., Song, L., Yu, W., Yang, H., & Ma, M. (2018). Global land surface temperature influenced by vegetation cover and PM 2.5 from 2001 to 2016. *Remote Sensing*, 10(12), 1–18. https://doi.org/10.3390/rs10122034

Soni, P. (2021). Effects of COVID-19 lockdown phases in India: an atmospheric perspective. *Environment, Development and Sustainability*, 0123456789. https://doi.org/10.1007/s10668-020-01156-4

Soydan, O. (2020). Effects of landscape composition and patterns on land surface temperature: Urban heat island case study for Nigde, Turkey. *Urban Climate*, 34(December 2019), 100688. https://doi.org/10.1016/j.uclim.2020.100688

Srbinovska, M., Andova, V., Mateska, A. K., & Krstevska, M. C. (2021). The effect of small green walls on reduction of particulate matter concentration in open areas. *Journal of Cleaner Production*, 279, 123306. https://doi.org/10.1016/j.jclepro.2020.123306

Tallis, M. J., Amorim, J. H., Calfapietra, C., & Smith, P. F. (2015). The impacts of green infrastructure on air quality and temperature. In *Handbook on Green Infrastructure: Planning, design and implementation* (Issue January 2016). https://doi.org/10.4337/9781783474004.00008

Thiis, T. K., Gaitani, N., Burud, I., & Engan, J. A. (2018). Classification of urban blue green structures with aerial measurements. *International Journal of Sustainable Development and Planning*, 13(4), 506–515. https://doi.org/10.2495/SDP-V13-N4-506-515

Tiwari, A., & Kumar, P. (2020). Integrated dispersion-deposition modelling for air pollutant reduction via green infrastructure at an urban scale. *Science of the Total Environment*, 723, 138078. https://doi.org/10.1016/j.scitotenv.2020.138078

Tomson, N., Michael, R. N., & Agranovski, I. E. (2025). Classic Theory of Aerosol Filtration for Application to Urban Green Infrastructure. *Water, Air, and Soil Pollution*, 236(3), 1–9. https://doi.org/10.1007/s11270-025-07829-y

UNDESA. (2019). World population prospects 2019. In *Department of Economic and Social Affairs. World Population Prospects* 2019. (Issue 141).

Urban Climate Lab. (2016). *The benefits of green infrastructure for heat mitigation and emissions reductions in cities*. June.

US EPA, OW, O. (2010). *What is Green Infrastructure?*

Vieira, J., Matos, P., Mexia, T., Silva, P., Lopes, N., Freitas, C., Correia, O., Santos-Reis, M., Branquinho, C., & Pinho, P. (2018). Green spaces are not all the same for the provision of air purification and climate regulation services: The case of urban parks. *Environmental Research*, 160(October 2017), 306–313. https://doi.org/10.1016/j.envres.2017.10.006

Vieira, L., Polisel, R., Ivanauskas, N., Shepherd, G., Waechter, J., Yamamoto, K., & Martins, F. (2015). Geographical patterns of terrestrial herbs : a new component in planning the conservation of the Brazilian. *Biodivers Conserv*, 24, 2181–2198. https://doi.org/10.1007/s10531-015-0967-8

WHO. (2018). *World Health Organization releases new global air pollution data | Climate & Clean Air Coalition*. 1–11. https://www.ccacoalition.org/en/news/world-health-organization-releases-new-global-air-pollution-data

Wu, H., Yang, C., Chen, J., Yang, S., Lu, T., & Lin, X. (2018). Effects of Green space landscape patterns on particulate matter in Zhejiang Province, China. *Atmospheric Pollution Research*, 9(5), 923–933. https://doi.org/10.1016/j.apr.2018.03.004

Wu, J., Xie, W., Li, W., & Li, J. (2015). Effects of urban landscape pattern on PM2.5 Pollution-A Beijing Case Study. *PLoS ONE*, 10(11), 1–20. https://doi.org/10.1371/journal.pone.0142449

Wu, X., Chen, Y., Guo, J., Wang, G., & Gong, Y. (2017). Spatial concentration, impact factors and prevention-control measures of PM2.5 pollution in China. *Natural Hazards*, 86(1), 393–410. https://doi.org/10.1007/s11069-016-2697-y

Yale and Columbia Universities. (2022). *Environmental Performance Index* (Vol. 1, Issue June).

Yang, H., Wu, M., Liu, W., Zhang, Z., Zhang, N., & Wan, S. (2011). Community structure and composition in response to climate change in a temperate steppe. *Global Change Biology*, 17(1), 452–465. https://doi.org/10.1111/j.1365-2486.2010.02253.x

Yao, M., Smith, M., & Peng, C. (2025). Modelling the effects of vegetation and urban form on air quality in real urban environments: A systematic review of measurements, methods, and predictions. In *Urban Forestry and Urban Greening* (Vol. 105). https://doi.org/10.1016/j.ufug.2025.128693

Yu, X., & Jingyi L, Y. H. (2019). A Review of the Relationship Between Urban Green Morphology and Urban Climate. *Urban Morphology Theory*, 23(10), 835–846.

Yu, Z., Wang, Y., Deng, J., Shen, Z., Wang, K., Zhu, J., & Gan, M. (2017). Dynamics of hierarchical urban green space patches and implications for management policy. *Sensors (Switzerland)*, 17(6). https://doi.org/10.3390/s17061304

Zhang, R., Chen, G., Yin, Z., Zhang, Y., & Ma, K. (2021a). Urban greening based on the supply and demand of atmospheric. *Ecological Indicators*, 126, 107696. https://doi.org/10.1016/j.ecolind.2021.107696

Zhang, R., Chen, G., Yin, Z., Zhang, Y., & Ma, K. (2021b). Urban greening based on the supply and demand of atmospheric PM2.5 removal. *Ecological Indicators*, 126, 107696. https://doi.org/10.1016/j.ecolind.2021.107696

Zhang, S., Ban, Y., Xu, Z., Cheng, J., & Li, M. (2016). Comparative evaluation of influencing factors on aquaculture wastewater treatment by various constructed wetlands. *Ecological Engineering*, 93, 221–225. https://doi.org/10.1016/j.ecoleng.2016.05.029

Zhang, X., Xi, Z., Li, X., Wang, C., Qiu, L., & Gao, T. (2024). Urban green space influencing air particulate matter concentration at different spatial scales base on land use regression model Urban green space influencing

air particulate matter concentration at different 2 spatial scales base on land use regression m. *Sustainability*, 3. https://ssrn.com/abstract=4684225

Zheng, D., Zhang, G., Shan, H., Tu, Q., Wu, H., & Li, S. (2020). Spatio-temporal evolution of urban morphology in the Yangtze River Middle Reaches Megalopolis, China. *Sustainability (Switzerland)*, 12(5), 1–15. https://doi.org/10.3390/su12051738

Zhou, W., Huang, G., & Cadenasso, M. L. (2011). Does spatial configuration matter? Understanding the effects of land cover pattern on land surface temperature in urban landscapes. *Landscape and Urban Planning*, 102(1), 54–63. https://doi.org/10.1016/j.landurbplan.2011.03.009

Zhou, W., Shen, X., Cao, F., Sun, Y., & Ph, D. (2019). *Effects of Area and Shape of Greenspace on Urban Cooling in Nanjing* , China. 145(4), 1–9. https://doi.org/10.1061/(ASCE)UP.1943-5444.0000520

Zhou, Y., Liu, H., Zhou, J., & Xia, M. (2019). GIS-based urban afforestation spatial patterns and a strategy for PM2.5 removal. *Forests*, 10(10), 1–17. https://doi.org/10.3390/f10100875